THE UNIVERSITY OF
SYDNEY

Identification and characterisation of a secreted acid phosphatase, Aph1 in the fungal pathogen *Cryptococcus neoformans*

So Young Cha

A thesis submitted in fulfilment of the requirements for the degree of Master of Philosophy (Medicine)

Department of Infectious Diseases and Immunology

Faculty of Medicine

University of Sydney

March, 2015

Disclaimer

I, hereby certify that the work presented in this thesis is original and was completed by the author, except where due acknowledgement has been made. The work was conducted while the author was enrolled in the Department of Infectious Diseases and Immunology at the University of Sydney and carried out at the Centre for Infectious Diseases and Microbiology, Westmead Hospital, NSW, Australia under the supervision of Dr. Julianne Djordjevic and Dr. Sophia Lev. I certify that this thesis has not already been submitted, wholly or in part, for any degree at any other university or institution and all help received in preparing this thesis, and all sources used, have been acknowledged.

_____ _____

So Young Cha Date

Acknowledgements

I would like to express my sincere gratitude to my supervisors, Dr. Julianne Djordjevic and Dr. Sophie Lev, whose expertise, understanding, and patience, added considerably to my Master's degree experience. Thank you Sophie for your provision and consistent support, especially in the laboratory. I appreciate all the help you have given me with your vast knowledge and skills. And Julie, thank you for your patience and dedication in going through my thesis. Thank you for all the times you have committed, giving me constructive advice, and enduring through the all the difficult times to push, and get me this far.

Thank you both for your guidance not only with the thesis, but also with many other aspects. You both have shown me what it is like to work with passion, and your dedication in everything you do has challenged and allowed to me re-evaluate my standards. But most of all, it has also inspired me to strive for more wherever I may be. It has been a challenging time, yet one I really enjoyed and am ever grateful for.

I would also like to thank Prof. Tania Sorrell for opening this opportunity, and for her encouragements throughout the course of my Masters.

And to Desmarini and Cecilia, all this would not have been possible without you guys. Des, thank you for all that you have done for me this year. I appreciate every help and advice you have given me. Your support in and out of the lab has made everything possible. I always knew I could rely on you. And Cecilia, the same goes for you. Thank you for caring for me with your supportive words and actions. I enjoyed spending time and getting to know you guys.

I would also like to thank and acknowledge all the other people who have supported and helped me along the way. Christabel Wilson and Chayanika Biswas for their friendly support, Steve Schibeci for his kind encouragements and help with cell cultures, Aziza Khan and Prof. Wieland Meyer for providing the larvae and Dr. Karen Byth for her assistance with the statistical analysis.

I would also like to take this opportunity thank my parents and family for their loving support. I know I don't express it often but I really appreciate all that you do for me. Thank you for supporting me even in your most difficult times.

Lastly, I would like to thank God. Thank you that you are faithful all the time. Thank you loving me, and constantly bringing me back to you. I hope to be the person you have set me to be.

Throughout the course of this thesis, not only have I learnt and become equipped with technical skills, I have also learnt many valuable life lessons that I know will help me become a better worker and person. And I would like to reiterate my thanks to my supervisors for this opportunity.

Contents

List of Tables

List of Figures

Abstract

Invasive fungal diseases (IFDs) are a major course of morbidity and mortality world-wide and new antifungals are urgently needed. IFDs caused by the human fungal pathogen *Cryptococcus neoformans* result in >625,000 deaths from meningoencephalitis annually in HIV-infected patients alone. *C. neoformans* is also a well-accepted fungal model used for studying pathogenesis mechanisms. It produces a range of virulence factors to enable it to cause disease, including a polysaccharide capsule and melanin. Extracellular acid phosphatase activity has been detected in over 95% of the *C. neoformans* strains isolated from patients with AIDS, including the highly-virulent serotype A reference strain H99. Acid phosphatase activity is produced by numerous microbes when free phosphate (Pi) is limited to release Pi from complex organic sources. However the contribution of this activity to the virulence of *C. neoformans* has never been determined.

As part of this study, a BLAST search of the *C. neoformans* H99 genome was performed using the secreted, Pi-repressible acid phosphatase, Pho5, from *Saccharomyces cerevisiae* as a query, and four uncharacterised acid phosphatases were identified: CNAG 02944 (Aph1), CNAG_06967 (Aph2), CNAG_02681 (Aph3) and CNAG_06115 (Aph4). Only Aph1 is predicted to be secreted. By creating an isogenic *APH1* gene deletion mutant strain *(Δaph1)* from H99 and comparing the two strains, the aims of this study were to determine (1) whether Aph1 is the secreted acid phosphatase responsible for the extracellular acid phosphatase activity in H99, and *APH1* responsiveness to Pi, (2) Aph1 substrate specificity (3) the role of Aph1 in fungal cellular function and virulence and (4) whether *APH2*, *APH3* and *APH4* are also Pi-responsive genes and whether their expression profile is altered in the absence of *APH1*. *APH1* gene deletion in *Δaph1* transformants was confirmed by the acquisition of neomycin resistance (since *APH1* coding sequence was replaced with a neomycin resistance gene (NEO^R)), by PCR amplification across the recombination junctions of the *APH1* deletion construct, and by the absence of extracellular acid phosphatase activity, as assessed using the chromogenic substrate para-nitrophenyl phosphate (pNPP).

To examine whether Aph1 production correlated with Pi availability, WT and *Δaph1* were incubated in the presence and absence of Pi and their secretions were assayed spectrophotometrically for acid phosphatase activity over an 80 min time course using pNPP. In contrast to WT, which produced acid phosphatase activity in the absence of phosphate,

Δaph1 produced almost no detectable extracellular acid phosphatase activity. This finding indicates that *APH1* gene product contributes all of the extracellular acid phosphatase activity in *C. neoformans,* and production of Aph1 is induced by Pi deprivation. Pi deprivation also induced *APH1* gene expression in WT, but not in *Δaph1,* as measured by qPCR. The ability of WT and *Δaph1* secretions to hydrolyse a broad range of phosphorylated substrates was compared using a malachite green assay. Phosphotyrosine (but not phosphoserine and phosphothreonine), glucose-1-phosphate, β-glycerol phosphate, adenosine monophosphate (AMP) and mannose-6-phosphate were all found to be substrates of Aph1. The absence of *APH1* in *Δaph1* did not compromise the growth of *C. neoformans* under normal and stress conditions, including human physiological temperature (37°C), its ability to produce melanin and capsule or its ability to grow in the absence of an external source of phosphate. However, *Δaph1* was less virulent in the *Galleria mellonella* (wax moth) and mouse inhalation models of cryptococcosis. The mechanism for the reduced virulence was unlikely to be due to a role for Aph1 in facilitating adhesion of *C. neoformans* to lung epithelium as indicated in previous studies by others, since WT and *Δaph1* bound to a lung epithelial cell line, A549, to a similar extent.

Expression of *APH2*, *APH3* and *APH4*, encoding intracellular acid phosphatases, was also investigated. Similar to *APH1*, *APH3* and *APH4*, and to a lesser extent *APH2*, were induced during Pi-deprivation in WT. To test the possibility that the intracellular acid phosphatases compensate for the lack of Aph1 in the *Δaph1* mutant, the expression of these genes in *Δaph1* under inducing (Pi-deficient) conditions was quantified. However, the expression of *APH2-APH4* in *Δaph1* was not higher than in WT, indicating that any potential compensation by *APH3* and *APH4* in the absence of *APH1* is not reflected at the transcriptional level.

In conclusion, Aph1 is the major secreted acid phosphatase in *C. neoformans* and similar to Pho5 from *S. cerevisae*, Aph1 production is regulated at the transcriptional level in response to Pi-availability. Similarly, expression of the other acid phosphatases, especially Aph3 and Aph4, is regulated by Pi availability, indicating that they are also components of the phosphate-responsive (PHO) system in *C. neoformans.* Aph1 contributes to the virulence of *C. neoformans* and this is most likely via its ability to release Pi from a broad range of physiological substrates, including potential immunomodulators, and to contribute to the maintenance of Pi homeostasis.

1 Introduction

1.1 The fungal kingdom

Fungi belong to one of the five kingdoms within the domain *Eukarya,* which include animals and plants. They exist in unicellular form (yeast) or in a filamentous form (mould) and are classified into phyla on the basis of their mode of sexual spore production (Prescott, 2005). Fungi have some unique features that distinguish them from animals: they possess a cell wall and their major sterol is ergosterol, rather than cholesterol. Although antifungal drugs have been designed to exploit these unique features, they have certain limitations which are discussed in more detail below.

Fungi are ubiquitous in nature and it has been estimated that up to 1.5 million fungal species exist, with approximately 90,000 species described to date (Prescott, 2005). In nature, fungi play an important role in decomposition and degradation of complex organic materials. Thus they are heterotrophic: obtain nutrients from external sources rather than by producing their own nutrition as in the case of auxotrophs (plants). They do this by secreting extracellular enzymes including phospholipases, proteases, cellulases and acid phosphatases. These enzymes break down the complex organic sources, yielding simple carbon, nitrogen and phosphorus sources for their nutrition and the nutrition of other soil-dwelling organisms including plants (Murray, 2009). Fungi are also important for the human food industry, particularly in the manufacture of wine and cheese, and for the production of antibiotics, as they synthesize penicillin and cyclosporine (Prescott, 2005). However, some fungal species can be pathogenic and cause diseases in plants, animals and humans, and hence are widely studied in order to understand the mechanisms they use to cause disease. Most fungi that cause disease in humans are ascomycetes (produce ascospores) e.g. *Candida* and *Aspergillus* species, while *Cryptococcus neoformans* and *Cryptococcus gattii* are basidiomycetes (produce basidiospores).

1.2 Medically significant fungi

Most fungal pathogens of medical importance are opportunistic, or secondary pathogens as a compromised host immune system is the major pre-disposing factor for the establishment of Invasive Fungal Disease (IFD). People who are most at risk of developing an IFD are those with a compromised immune system, such as HIV patients, organ transplant

recipients taking immunosuppressive agents or corticosteroids, those with blood cancers (e.g. Leukemia) receiving chemo- or radio-therapy, and those with inherited severe immunodeficiency (Park *et al.*, 2009), (Sun *et al.*, 2002), (Klock *et al.*, 2009), (Baddley *et al.*, 2011). Examples are *Aspergillus fumigatus*, *Candida albicans* and *Cryptococcus neoformans,* which cause the majority of cases of IFD (Prescott, 2005). Treatment of *Candida* and *Aspergillus* costs approximately 1.1 million/year in a single Australian haematology unit (Slavin *et al.*, 2004). Estimates of the monetary cost of treating infections due to *Cryptococcus neoformans* in developing countries such as Sub-Saharan Africa and South East Asia are more difficult to calculate. However, the human cost is enormous (see below). In addition to the secondary pathogens there are a few fungi which are sufficiently virulent to be considered as primary pathogens; they cause IFD in immunocompetent as well as in immunocompromised individuals. Thus a compromised immune system is not a predisposing factor for these pathogens to cause IFD. These primary pathogens are able to avoid or subvert the normal host defence mechanisms and multiply within the host to cause IFD (Murray, 2009). Examples include *Coccidioides immitis, Histoplasma capsulatum* and *Cryptococcus gattii*. A recent outbreak of cryptococcosis in immunocompetent individuals in Vancouver Island, British Columbia, was caused by *Cryptoccous gattii* and resulted in 200 cases of infection and 8 deaths (Fyfe *et al.*, 2008).

1.3 Antifungal treatments and their limitations

Treating IFD is challenging as fungal and mammalian cells are both eukaryotic and therefore biologically similar. However, as mentioned above, fungi do have some differences, including a cell wall and a different major sterol (ergosterol), which have been exploited for development of two major classes of antifungal drugs: those targeting fungal ergosterol (Amphotericin B: AMB) or enzymes in the ergosterol biosynthetic pathway (terbinafine and azoles) and enzymes involved in cell wall biosynthesis (the echinochandins). A third class inhibits DNA/RNA synthesis and interferes with ribosomal protein synthesis (5-fluorocytocine: 5-FC). Despite the development of these fungal target-specific drugs, these agents still have limitations.

Azole-based antifungal agents, such as fluconazole, inhibit a key enzyme in the ergosterol biosynthetic pathway encoded by *ERG11.* Inhibition of Erg11 leads to the exhaustion of cellular ergosterol and the accumulation of toxic ergosterol precursors, which

when substituted for ergosterol in the fungal membrane, alter membrane structure and function (Ghannoum & Rice, 1999). In contrast to AMB, which is fungicidal, azoles are fungistatic, and can therefore lead to the development of resistance. Azoles however are less toxic than AMB and are therefore safer to use. Examples of acquired resistance to cryptococcal infections are found in developing countries where access to Highly Active Antiretroviral Therapy (HAART) and the full cohort of antifungal agents used in combination therapy is limited due to cost. In developed countries, drug resistance is minimized in patients with infections caused by *C. neoformans* by treating with a combination of AMB and 5-FC for the first two weeks, followed by a switch to the fungistatic azoles. However, in developing countries like Sub-saharan Africa, the cheaper azole drugs are often used inappropriately as a monotherapy and this has led to the development of resistance. Some fungal species (e.g. Scedosporium species) can also be inherently azole resistant.

Long term use of AMB can lead to side-effects including hepatic and renal toxicity, or produce adverse effects when used in combination with other antimicrobials (Shapiro *et al.*, 2011). Additionally, some antifungals do not exhibit broad specificity across fungal species. For example, the Echinocandin group targeting the cell wall, although well-tolerated, are ineffective in treating cryptococcal infections. Morbidity and mortality from IFD can be decreased by making an early diagnosis so that treatment can start sooner. An example is cryptococcal meningitis which is fatal without treatment, with only 20% mortality even when appropriate treatment is received. Early detection of cryptococcal antigen with the Dip stick test can therefore improve the prognosis (Jarvis *et al.*, 2011). In summary there is an urgent need to develop safer and more effective antifungals. Knowledge of the mechanisms of fungal development and pathogenicity is essential for development of novel antifungal drugs.

1.4 *Cryptococcus neoformans*– an important human pathogen and fungal model

C. neoformans is an opportunistic fungal pathogen causing approximately one million cases of infection and >600,000 deaths annually in HIV-infected patients alone (Park *et al*., 2009) and there are more deaths from cryptococcal meningo-encephalitis in Sub-Saharan Africa than there are from tuberculosis (Park *et al*., 2009). *C. neoformans* mainly affects people who are immunocompromised but can also affect people with a competent immune system. Although such infections are rare, it has been reported that ~10% of patients

presenting with cryptococcal meningo-encephalitis in Vietman do not have HIV (Chau *et al.*, 2010). *C. neoformans* is the leading cause of fungal meningo-encephalitis worldwide. *C. gattii* on the other hand does not have as great a tendency to disseminate to the CNS and cause meningo-encephalitis, and is more geographically restricted than *C. neoformans.*

C. neoformans is ubiquitous, with the main reservoir of infectious particles (spores or small desiccated yeast cells) being pigeon excreta, trees and soil. The infectious particles enter the host via the nasal passages after being inhaled from the environment (Figure 1.1.). Normally if the patient is immunocompetent, the infection is cleared from the lungs or potentially may reside in a dormant state inside macrophages within the lymph nodes. If the patient is immunocompromised, the pathogen can propagate in the lung tissue and cause pneumonia. From the lungs it can disseminate to the central nervous system (CNS) via the blood and lymphatic system to cause meningo-encephalitis. *C. neoformans* can survive and replicate in the extracellular environment (e.g., alveolar spaces, bloodstream) or it is engulfed by phagocytic cells (such as macrophages). Once inside phagocytic cells, *C. neoformans* can survive and replicate in the acidic phagolysome or it can be expelled back into the neutral/alkaline extracellular space without killing the host cells (Nicola *et al.*, 2011). *C. neoformans* has also been found in the blood which is also of a more neutral pH.

In addition to being a pathogen of medical relevance, many factors make *C. neoformans* an excellent model in which to study fungal pathogenesis. Firstly, its genome has been sequenced (Loftus *et al.*, 2005). Secondly its genome is haploid and highly amenable to genetic manipulation, with protocols for carrying out targeted gene deletion, mRNA suppression and chromosomal and episomal gene expression being well-established. Thirdly, robust animal models of cryptococcal infection are well developed (Casadevall, 1998).

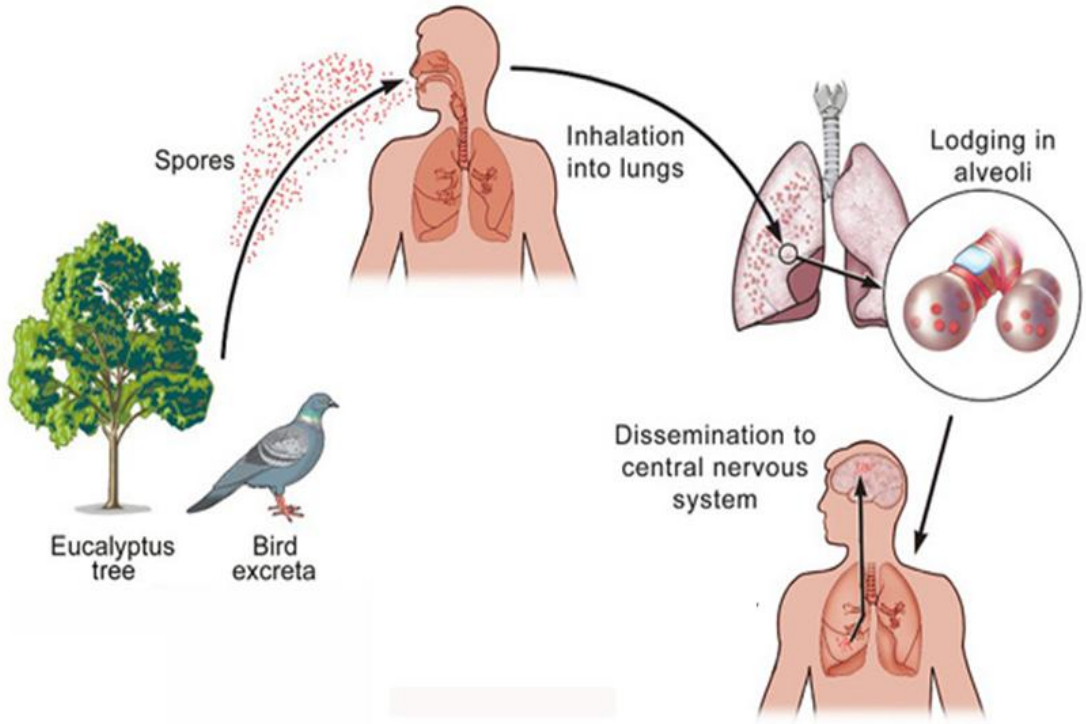

Figure 1.1 Route of *C. neoformans* infection in the mammalian host.

(Modified from (Hull & Heitman, 2002)). The infectious propagules are spores or small desiccated yeast cells. The main reservoirs for infectious propagules are soil, trees and pigeon excreta. Infectious propagules are inhaled from the environment and lodge in the alveoli. The yeast can then infect the lungs, causing pneumonia. From the lungs it can disseminate to the CNS via the blood and lymphatic system to cause meningo-encephalitis.

1.5 *C. neoformans* virulence factors

The virulence of a pathogen is defined as its infectiousness, or its ability to cause disease. Several factors contribute to the virulence of *C. neoformans*, including the ability to grow at host temperature (37˚C) and produce phospholipase B1, melanin and a polysaccharide capsule. Additional virulence-related traits include the production of the rigid cell wall and the ability to grow intracellularly (namely, inside macrophages). For a gene to be labelled as “associated with virulence”, it must satisfy the criteria defined by the “molecular Koch’s postulates”. These criteria include that (1) the phenotype associated with the gene in question is associated with pathogenic microbial species, (2) inactivation of the gene responsible for the pathogenic phenotype results in decreased virulence, and (3) restoration of the intact gene is associated with reversion to wild-type virulence (Falkow, 1988).

1.5.1 Growth at host temperature (37°C)

In order for the fungi to thrive inside the host, they must be able to adapt to the host temperature. Several sensing and adaptation mechanisms have been identified in *C. neoformans*. These include the calcineurin and RAS signalling pathways (Nichols *et al.*, 2007), (Waugh *et al.*, 2002), (Kraus *et al.*, 2005, Alspaugh *et al.*, 2000). Our laboratory has demonstrated significance of the enzyme phospholipase C1 (PLC1) for growth of *C. neoformans* at physiological temperature (Chayakulkeeree *et al.*, 2008).

1.5.2 Melanin

In the presence of a suitable precursor and a poor nutritional environment, *C. neoformans* produces an extracellular, black, negatively charged pigment melanin (Williamson, 1994), (Casadevall *et al.*, 2000). Melanin supports the cryptococcal cell wall, and is protective against host-derived oxidative stress, extreme temperature, UV irradiation and phagocytosis by host macrophages (Casadevall *et al*., 2000, Casadevall, 1998). Melanin is produced from host- or soil-derived phenolic compounds, for example epinephrine and L-dopa, and its biosynthesis is catalysed by a cell wall associated enzyme laccase. Laccase is therefore an important virulence factor of *C. neoformans* (Salas *et al.*, 1996, Pukkila-Worley *et al.*, 2005, Williamson, 1994)

1.5.3 Polysaccharide capsule

The most unique virulence factor of *C. neoformans* is the extracellular polysaccharide capsule, which also determines cryptococcal serotype. The two main capsule components are the polysaccharides glucuronoxylomannan (GXM) and glucuronoxylomannogalactan (GXMGal); GXM accounts for 90-95% of the capsule's mass (Zaragoza *et al.*, 2009). Capsule formation is induced under environmentally stressful conditions to protect cryptococcal cells from environmental challenges and desiccation. During host infection, the capsule protects *C. neoformans* from engulfment by macrophages and enables cryptococcal cells to evade the immune response by shielding cell wall antigens. Moreover, the capsule affects cytokine production, inhibits leukocyte migration to cryptococcal infection sites and depletes components of the complement in the host. It also assists *C. neoformans* to disseminate from the lungs to the CNS (Vecchiarelli & Monari, 2012), reviewed in (Garcia-Rodas *et al.*, 2011). Polysaccharide capsule is a dynamic structure that can change in size

and undergoes rearrangement during budding (McFadden *et al.*, 2006). Changes in capsular structure are also associated with phenotypic switching in *C. neoformans* (Guerrero & Fries, 2008, Jain *et al.*, 2006b). Alteration from a smooth to a mucoid colony phenotype, associated with increased production of capsular material, caused hypervirulence and increased intracerebral pressure in a rat model of cryptococcal meningitis (Fries *et al.*, 2005, Jain *et al.*, 2006a)

1.5.4 Phospholipases

Phospholipases are a group of enzymes that hydrolyse one or more ester linkages in the phospholipid backbone of glycerophospholipids. Phospholipases are categorised into 5 groups based on the ester bond that they cleave: A1, A2, B, C, and D (reviewed in (Ghannoum, 2000)).The two major phospholipases associated with the virulence of *C. neoformans* are phospholipase B (PLB1) (Chen *et al.*, 2000) and phospholipase C (PLC1) (Chayakulkeeree *et al* 2007) reviewed in (Djordjevic, 2010). In *C. neoformans*, PLB1 is a secreted protein (Djordjevic *et al.*, 2005), (Siafakas *et al.*, 2007), (Siafakas *et al.*, 2006)). PLB1 has three catalytic activities directed towards its major substrate, phosphotidylcholine (PC): phospholipase B (PLB) lysophospholipase (LPL) and lysophospholipase-transacylase (LPTA) (Chen *et al*., 2000). The PLB and LPL activities cleave fatty acids from a phospholipid and lysophospholipid respectively, while the LPTA activity transfers a free fatty acid to a lysophospholipid to produce a phospholipid.

1.6 Acid phosphatases

1.6.1 Phosphate utilization by fungi and the role of Acid Phosphatase

Phosphorus in the form of inorganic phosphate (Pi) is an essential nutrient for all living things. Intracellular Pi is essential for the synthesis of macromolecules, including ATP, phospholipids, and proteins, and is involved in numerous signalling and metabolic processes. In order to synthesize these molecules, millimolar concentrations of phosphate are needed in the cytoplasm, while most environmental Pi concentrations are considerably lower. Acid phosphatases are a family of enzymes that catalyse the hydrolysis of phosphate monoesters bound up in complex organic sources, releasing free Pi. They work optimally in acidic

conditions (pH 4.5-5.5) (Anand & Srivastava, 2012). To concentrate Pi inside the cytoplasm, fungi deploy membranal Pi transporters to transport Pi into the cell (Wykoff & O'Shea, 2001).

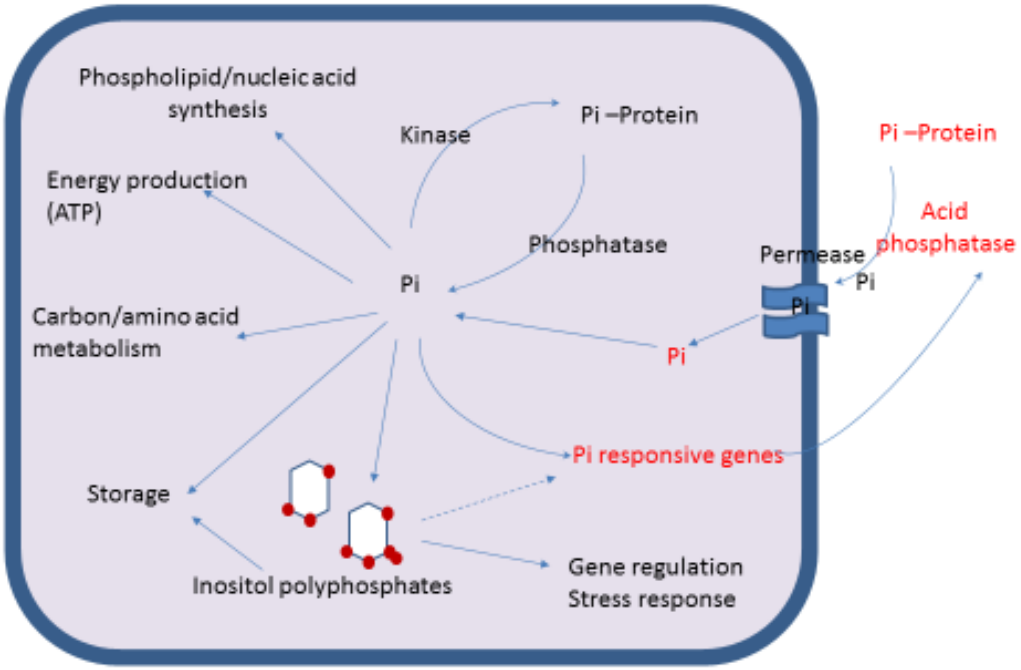

Figure 1.2 Phosphate homeostasis is essential for cellular function.

When intracellular phosphate is low, Pi responsive genes are induced to produce secreted acid phosphatase and other proteins involved in Pi mobilization, such as phosphate transporters. Secreted acid phosphatase frees up Pi from complex organic sources which are too big to cross the membrane and cell wall. This free Pi is transported across the membrane and cell wall via the transporters and mixes with the intracellular pool of Pi. Intracellular Pi is either stored (as polyphosphate) or used in the various physiological processes depicted. High intracellular Pi also shuts down the expression of secreted acid phosphatase and the Pi transporters.

1.6.2 The PHO pathway in the model yeast *Saccharomyces cerevisiae*

In the model non-pathogenic yeast, *S. cerevisiae*, Pi homeostasis is regulated by the phosphate (PHO) signal transduction pathway (PHO pathway). The PHO pathway consists of 3 main components (1) the PHO regulation system which is a signalling cascade comprised of kinases and transcription factors, which up or down-regulate the PHO responsive genes

according to the level of intracellular Pi (Tomar & Sinha, 2014); (2) PHO responsive genes, including secreted acid phosphatase Pho5 and a membrane transporter system comprising low- and high affinity Pi transporters, which allow *S. cerevisiae* to internalize extracelluar Pi and (3) Pho-responsive genes encoding enzymes involved in utilizing intracellular polyphosphate reserves. The PHO pathway receives and responds to signals from both the extra and intracellular environment and functions to maintain Pi homeostasis and to optimize Pi uptake and utilization. It is activated during Pi starvation (Oshima, 1997) (Figure 1.3).

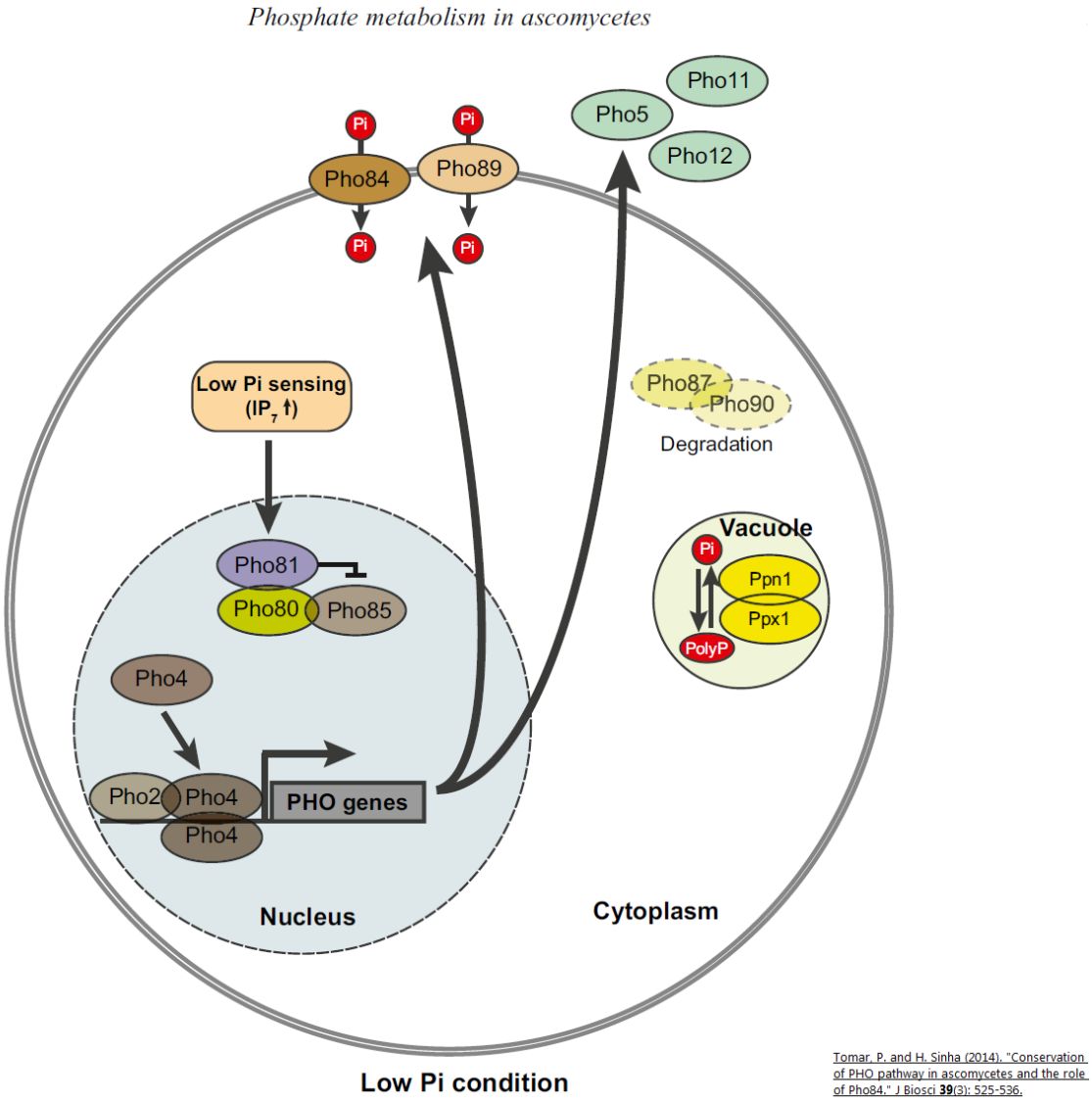

Figure 1.3: The PHO pathway is activated in low phosphate conditions.

In *S. cerevisiae*, the PHO regulation system consists of the cyclin-dependent kinase inhibitor, Pho81, the cyclin - cyclin-dependent kinase complex, Pho80-Pho85 and the transcription factors, Pho4 and Pho2. Under low-Pi conditions, Pho81 represses the Pho80-Pho85

complex, which in turn leads to hypo-phosphorylation of the transcription factor Pho4. Hypo-phosphorylation Pho4 in turn activates PHO genes, including the high affinity transporters (Pho84, Pho89) and secreted acid phosphatases (Pho5, Pho11 and Pho12). (Lenburg & O'Shea, 1996), (Oshima, 1997), (Persson *et al.*, 2003).

1.6.3 Classification of acid phosphatases, substrate specificity and function

Most acid phosphatases belong to the histidine phosphatase superfamily, which have a conserved catalytic core centred on a histidine (Rigden, 2008). The histidine phosphatase superfamily is divided into two branches. The 'phosphoglycerate mutase family' forms branch 1, while branch 2 contains mainly the 'acid phosphatases and phytases' (Rigden, 2008), which remove phosphate from inositol phytate/hexakisphosphate/IP_6. Phytate is the major storage form of phosphorus in soil and plants, and exists primarily as a complex with Ca^{2+}, Fe^{2+}, and Zn^{2+}, which are cations important in nutrition. Thus, phytase-mediated hydrolysis of phytate leads to the formation of less complex inositol phosphates and inositol, and thus increases the bioavailability of Pi and minerals important for growth and development of plants and animals. Eukaryotic Minpp1 (multiple inositol-polyphosphate phosphatase 1) regulates the cellular concentration of inositol pentakisphosphate (IP_5) and IP_6 (Chi *et al.*, 2000).

Branch 2 acid phosphatases include bacterial and eukaryotic enzymes. In *E. coli*, periplasmic glucose-1-phosphatase is required for growth on glucose 1-phosphate as a sole carbon source (Pradel & Boquet, 1991). Human prostatic acid phosphatase (PAP) hydrolyses lysophosphatidic acid in seminal plasma (Tanaka *et al.*, 2004). Phosphorylation and signalling of the receptor tyrosine kinase, ErbB2, can be regulated by prostatic acid phosphatase (Anand & Srivastava, 2012). Another acid phosphatase, ACPT, acts as a tyrosine phosphatase to modulate ErbB4 receptor-mediated signalling important for neuronal development and synaptic plasticity (Fleisig *et al.*, 2004). Tartrate-resistant acid phosphatase, TRAP, plays role in primary immune responses and bone remodelling (Anand & Srivastava, 2012). In the fission yeast *Schizosaccharomyces pombe*, production of a cell-surface acid phosphatase is repressed by thiamine suggesting a role in thiamine metabolism, possibly in the cleavage of a thiamine phosphate (Rigden, 2008).

An important functional characteristic of an enzyme is its catalytic activity towards different substrates and its substrate specificity (Anand & Srivastava, 2012). Depending on

the range and type of substrate it is able to catalyse, we are able to make assumptions of its biological and physiological significance and/or determine its role. Acid phosphatases are known to be able to catalyse a wide range of physiological substrates including energy storage molecules and phosphorylated sugars and amino acids (Anand & Srivastava, 2012).

1.6.4 Role of acid phosphatases in microbial pathogens

Extracellular acid phosphatases are produced by many microbial species, including the bacterial pathogens, *Mycobacterium tuberculosis* (Puri *et al.*, 2013) and *Legionella micdadei* (Saha *et al.*, 1988), the protozoan parasites, *Leishmania donovani* (Shakarian *et al.*, 2002) and *Trypanosoma cruzi* (Meyer-Fernandes *et al.*, 1999) and the fungal pathogens *Candida albicans* (Portela *et al.*, 2010), *Candida parapsilosis* (Kiffer-Moreira *et al.*, 2007a), *Sporothrix schenckii* (Arnold *et al.*, 1986), *Aspergillus fumigatus* (Bernard *et al.*, 2002), *Fonsecaea pedrosoi* (Kneipp *et al.*, 2003, Kneipp *et al.*, 2004), *Rhinocladiella aquaspersa* (Kneipp *et al.*, 2012), *Pseudallescheria boydii* (Kiffer-Moreira *et al.*, 2007b), *Paracoccidioides brasiliensis* (Xander *et al.*, 2007) (for review see (Gomes *et al.*, 2011)) and *Cryptococcus neoformans* (Vidotto *et al.*, 2006).

Secreted acid phosphatase (SAP) produced by *M. tuberculosis* is essential for pathogenesis and allows the bacteria to evade detection by the host immune system by preventing maturation of the macrophage phagosome (Puri *et al*., 2013). Interestingly, SAP is more homologous to fungal acid phosphatases than to those of bacterial origin, suggesting that the encoding gene has been acquired from fungi during the bacterial evolutionary process, and further highlighting the importance of fungal acid phosphatases in microbial pathogenesis. *Legionella micdadei*, which has adjusted to survive and multiply within phagocytic cells, was shown to block superoxide anion production by human neutrophils, possibly via hydrolysis of neutrophil derived phosphatidylinositol 4,5-bisphosphate and its secondary messenger hydrolysis product, IP_3 (Saha *et al*., 1988). Similarly, constitutively-expressed surface acid phosphatase produced by the protozoan, *L. donovani,* which also resides and multiplies within macrophage phagolysosomes, inhibited superoxide anion production by human neutrophils (Remaley *et al.*, 1984) (Shakarian *et al*., 2002).

In the fungal pathogens *Candida parapsilosis* (Fernanado *et al.*, 1999, Kiffer-Moreira *et al*., 2007a) *Fonsecaea pedrosoi* (Kneipp *et al*., 2003, Kneipp *et al*., 2004)) and *Rhinocladiella aquaspersa* (Kneipp *et al*., 2012), surface acid phosphatase activity contributes to adhesion of the fungal cells to the host cells, a process essential for subsequent infection. The phosphorylation and dephosphorylation of serine, threonine and tyrosine residues in extracellular domains of functionally important surface proteins of the host may be a mechanism defining the outcome of host-pathogen interaction (Belanger *et al.*, 2002).

Extracellular acid phosphatase activity has also been detected in over 95% of 310 *C. neoformans* strains isolated from AIDS patients in 5 different countries (Vidotto *et al*., 2006), suggesting that acid phosphatases may also be associated with cryptococcal virulence. (Collopy-Junior *et al.*, 2006) demonstrated that adhesion of *C. neoformans* cells to animal epithelial cells was reduced following non-specific irreversible inhibition of acid phosphatase activity by sodium orthovanadate. However, the enzymes responsible for this activity were never identified.

Thesis Aims

The overall aims of this thesis are to determine whether acid phosphate (Aph1) is responsible for the extracellular acid phosphate activity produced by a strain of *Cryptococcus neoformans* (H99) isolated from a patient with AIDS, characterise its mode of regulation and function, and determine its contribution to fungal virulence.

The specific aims are to:

1. Delete the *APH1* gene, which is predicted to encode a secreted protein (Aph1), using a targeted gene deletion strategy, to create the strain *Δaph1.*

   Then, by comparing the phenotypes of WT and *Δaph1,* determine:
2. Whether Aph1 contributes to extracellular acid phosphatase activity using a chromogenic assay ;
3. Whether Aph1 transcription and secretion is regulated by Pi availability;
4. Which phosphorylated substrates Aph1 hydrolyses
5. Whether Aph1 is essential for production of cryptococal virulence traits (melanin, capsule and ability to grow at human physiological temperature 37°C), resistance to stress and growth in the absence of an external source of phosphate
6. Whether Aph1 contributes to pathogenesis using wax moth and mouse inhalation infection models
7. Whether Aph1 facilitates adhesion of *C. neoformans* to a lung epithelial cell line
8. The effect of *APH1* absence on the expression of other APase-encoding genes and whether these genes are also regulated at the transcriptional level by Pi availability.

2 Material and Methods

2.1 General Reagents, Media and Stock Solutions

2.1.1 Preparation of Media and Stock Solutions

Procedures for all media and stock solutions are listed in Appendix 1. Water acquired from the Milli-Q Integral Water Purification System (EMD Millipore Corporation, MA, USA) was used to prepare all media and stock solutions. pH of media and solutions was determined using a pH meter. All media were sterilised by autoclaving and all stock solutions were filter sterilised through a 0.22 µM filter (Appendix 2).

2.1.2 Commercial Reagents

All commercially available products, kits, chemicals, enzymes and antibodies used in this thesis are listed in Appendix 2.

2.2 Strains

The *Cryptococcus neoformans* strain used for all experimental work in this thesis was *Cryptococcus neoformans var. grubii H99* (serotype A); (https://www.broadinstitute.org/annotation/genome/cryptococcus_neoformans/MultiHome.html) (Mitchell *et al.*, 1995). This strain is referred to as wild type (WT) H99 and was used to create the *APH1* deletion mutant.

WT H99 and the *APH1* gene deletion mutant strain (Table 1) were cultured from frozen 20% glycerol stock on Sabouraud Dextrose Agar (SAB) (Appendix 2) plates at room temperature (RT) for 72 hours. Plates were stored inverted at 4°C. Fresh cultures were prepared from frozen glycerol stocks weekly to fortnightly.

Table 1. Strains used in this thesis

Strain	Serotype	Name	Genotype
H99	A	WT	H99 WT
H99	A	*Δaph1*	*Δaph1:NEO*

***The coding region of the *APH1* gene has been replaced by the NEO resistance cassette.**

2.3 Polymerase Chain Reaction (PCR)

PCR Amplification from Genomic DNA

PCR reactions (for construction of the deletion construct and verifying targeted gene deletion) were performed using genomic DNA extracted from *C. neoformans* as a template and the high-fidelity *TaKaRa Ex Taq* polymerase enzyme (Appendix 2). The PCR mixture (50 µl) was prepared in a 0.2 ml PCR tube as follows: 0.25 µl of *TaKaRa Ex Taq* (5 units/µl), 5 µl of 10X *Ex Taq* Buffer, 4 µl of dNTP Mix (2.5mM each), 2.5 µl each of forward and reverse primer (20 µM), 1 µl of DNA template (100-500 ng) and 34.75 µl of UltraPure water. The final concentrations of each dNTP and each primer were 0.2 mM and 1 µM, respectively. The thermal cycler (Biometra, Goettingen, Germany) was initially set up as shown below, with the annealing temperature and/or extension temperature altered when applicable depending on the primers and PCR product size.

Initial denaturation	95°C 5 min	
Denaturation	95°C 30 sec	35 cycles
Annealing	55°C 30 sec	
Extension	72°C 1 min/kb of PCR product	
Final extension	72°C 10 min	

To visualize the PCR products, the PCR mixtures were subjected to agarose gel electrophoresis as described in section 2.4.

2.4 Agarose Gel Electrophoresis and Visualization of DNA

DNA including PCR products were visualized by agarose gel electrophoresis and SYBR Safe DNA gel staining (Appendix 2). The agarose gel was prepared by dissolving 1.5% (w/v) agarose (Appendix 2) in 1X Tris-borate-EDTA (TBE) buffer (Appendix 2) by heating in a microwave oven, following by the addition of 1µL SYBR Safe DNA Gel stain per 10ml of liquid agarose gel and pouring of the gel into a gel tray containing a comb. When the gel had cooled and solidified, the comb was removed and the entire casting tray was lowered into SUB-CELL GT electrophoresis tank (Bio-Rad Laboratories Pty. Ltd., NSW, Australia) and covered with TBE buffer. A total of 10 µl of the PCR reaction was mixed with 2 µl of 6X

Blue/Orange Loading Dye (Appendix 1) and loaded into each well of the agarose gel. To determine the size of the DNA fragments, 10 µl (1 µg) of 1kb DNA Ladder (Appendix 2) were loaded into a well of the same agarose gel before electrophoresis was started. Gel electrophoresis was performed by applying an electric current to the tank at 100 V for 1 h (may vary depending on the product size). Product was then visualized using a Safe Imager blue light transilluminator (Invitrogen, CA, USA).

2.5 Extraction of *C. neoformans* Genomic DNA

C. neoformans strains (WT or ∆*aph1)* were cultured at 30°C for 3 days on YPD agar. Approximately 2-3 loopfuls of yeast cells were transferred from the plates to a 2-ml screw-capped microfuge tube containing 0.5 ml of acid-washed glass beads (0.5 mm in diameter) and 0.5 ml of TENTS buffer (see Appendix 2). The tubes were vortexed vigorously for 2 x 30 sec with a 1 min cooling period on ice in between each vortex and following the final vortex. Five hundred µl of phenol:chloroform:isoamyl alcohol (IAA) (25:24:1) was added to each tube followed by vigorous vortexing as above. The tubes were centrifuged at maximum speed at 4°C for 15 min to achieve a phase separation. The supernatants were transferred to a fresh microfuge tube and 500 µl of phenol:chloroform:IAA (25:24:1) was added followed by vigorous vortexing for 30 sec. The tubes were centrifuged as above to achieve phase separation, the supernatants were transferred to a fresh microfuge tube and 500 µl of chloroform was added, followed by vortexing. The tubes were centrifuged as above to achieve phase separation and the supernatants (approximately 500 µl) were transferred to a fresh microfuge tube. DNA precipitation was achieved by adding 50 µl of 3M sodium acetate (1/10 volume) and 1.25 ml of absolute ethanol (2.5 volume). The tubes were incubated at 4°C for at least 1 hour or overnight. The tubes were centrifuged as above to collect the precipitated DNA and the pellets were washed once with 70% ethanol. Finally, DNA was re-suspended in TE buffer (Appendix 2) or 10 mM Tris (pH 7.5) and used for PCR as described above.

2.6 Targeted Deletion of the *APH1* Gene in *C. neoformans*

2.6.1 Construction of an *APH1* deletion construct by overlap PCR

APH1 (CNAG 02944) was selectively deleted in *C. neoformans* strain H99 (Wild-Type, WT). This was achieved by making an *APH1* gene deletion construct *in vitro* using overlap PCR, and introducing it into WT *C. neoformans* using biolistic transformation where it could replace the native *APH1* gene by homologous recombination. All PCR amplifications were performed using a high-fidelity polymerase *ExTaq* (Appendix 2) as described in section 2.3. To create the deletion construct, genomic DNA from *C. neoformans* was prepared as described in section 2.5, and flanking sequences upstream (5'flank, 787bp) and downstream (3'flank, 952 bp) of the coding region of the APH1 gene (designated as CNAG_02944 in the *C. neoformans* H99 serotype A genome database) were amplified by PCR in separate reactions, using primer pairs APH1-1F/APH1-2R and APH1-3F/APH1-4R respectively (Section 2.2, Table 1). Simultaneously, and in a separate reaction, the neomycin resistance (NEO^R) cassette was amplified from the pJAF vector using primers NEOF and NEOR (Figure 3.3 and Section 2.6.2, Table 2.). Each PCR product was confirmed to be of the correct size using electrophoresis on a 0.8% agarose gel and SYBR safe staining, as described in section 2.4, and then purified using a Promega Gel Extraction Kit. The three purified PCR products (5' flank, Neo^r cassette and 3' flank), which contained overlapping ends, were combined in a single tube to provide a template for overlap PCR using primers APH1-1F/APH1-5R (Figure 3.3, Section 2.6.2, Table 2.). The final product, which was approximately 3 kb in size, was gel-purified as described above for the single PCR products, and used to transform strain H99 using a biolistic DNA delivery protocol (section 2.6.2).

2.6.2 Biolistic Transformation

The delivery of the *APH1* deletion construct into the WT *C. neoformans* (H99) strain was achieved by biolistic transformation using the method of (Toffaletti *et al.*, 1993) with minor modifications. Ten ml of an overnight YPD culture of H99 was concentrated to approximately 300 µl by centrifugation and spread onto a YPD agar plate containing 1 M sorbitol. The following reagents were added to 200 ng of the gel-purified deletion construct prepared in 2.6 (the amount used for one bombardment) with continuous mixing and in the following order: 10 µl of 0.6 µm gold bead microcarrier suspension (Appendix 2), 10 µl 2.5M

$CaCl_2$ and 2 µl 1M spermidine. The amount of DNA and reagents were scaled up accordingly when more than one bombardment was carried out. The DNA was allowed to precipitate onto the beads for 10 min without agitation. The DNA-coated gold beads were pelleted by centrifugation, the supernatant was removed and the pellet washed with 250 µl absolute ethanol. The final pellets were resuspended in 10 µl absolute ethanol per bombardment. For each bombardment, 10 µl of the DNA/gold bead suspension was spread onto the centre of the macrocarrier disc and allowed to dry. Particle delivery from the macrocarrier disc to the cell culture lawn was carried out using the biolistic PDS-1000/He system (Bio-Rad Laboratories Pty. Ltd., NSW, Australia) once the vacuum in the chamber had reached 28.5 inches Hg. Activation of the firing mechanism allowed the pressurized helium gas to break the 1350-psi rupture disk, generating a helium shockwave into the bombardment chamber. The shock wave hits the macrocarrier disc and propels the adhered DNA-coated gold bead microcarriers toward the target cells. A stopping screen placed between the macrocarrier assembly and the target cells, retains the macrocarrier, allowing the DNA-coated gold microprojectiles to pass through and transform the target cells on the agar plate. After bombardment, the plate was incubated at 30^{o}C for 2-3 hours to allow recovery. The transformed cells in the middle of the plate (having an orange appearance due to the gold beads) where then dislodged with a scraper, mixed with 1 ml of 1M sorbitol and spread onto a selective YPD agar plate containing 100 µg/ml of geneticin (G418)/neomycin. The plate was incubated for 4-5 days at 30^{o}C to allow the transformants to grow. The colonies that grew were transferred to fresh YPD agar plates without the selective drug and subcultured a further 3 times in non-selective medium before being inoculated back onto YPD/G418 agar. Mitotically-stable transformants were screened for the absence of extracellular acid phosphate activity as described in 2.7.1. (Figure 3.4.) and by PCR as described in 2.3 (Figure 3.5) to confirm that the deletion construct had undergone homologous recombination into the native *APH1* locus. PCR-verified transformants were designated *Δaph1*.

Table 2. List of primer sequences used for *C. neoformans APH1* gene deletion

Primer	Type	Sequence
APH1-1F	Forward	5'-CAGCCGGGAAGAGATAA-3'
APH1-2R	Reverse	5'CTCCAGCTCACATCCTCGCAGGACGGTGTTTTTGGGTGAGT-3'
APH1-3F	Forward	5'-CCTCAGGATCTTCATGGCTCCTTATGGGCGTGCTCCTC-3'
APH1-4R	Reverse	5'-CCCTCTGCTCCATACGATTT-3'
APH1-OTS5'	Reverse	5'-CCTCTTGTAGCCGACGAATAAAT-3'
APH1-OTS3'	Reverse	5'-GAATCACCACACTCGACGCG-3'
NEOF	Forward	5'-CATGCAGGATTCGAGTGGCATG-3'
NEOR	Reverse	5'-GGAGCCATGAAGATCCTGAGGA-3'

2.7 Acid phosphatase activity assay using para-nitrophenol phosphate (pNPP)

2.7.1 Screening neomycin-resistant transformants for lack of extracellular acid phosphatase activity to identify Δ*aph1* mutants

Each transformant was inoculated into 100 μl phosphate-deficient (inducing) medium MM-KCl (0.5% KCl, 15 mM glucose, 10 mM $MgSO_4.7H_20$, 13 mM glycine, 3.0 uM thiamine) to maximize the production of acid phosphatase, and grown overnight in a 96 well plate. The chromogenic substrate, pNPP (50 mM Stock) was then added to each well to a final concentration of 10 mM and incubation was resumed at 37°C for 20 min. The reactions were stopped by addition of 50 μl of saturated Na_2CO_3. Wells containing mutants that had not turned yellow (remained clear) were considered as candidate *APH1* gene deletion mutants.

2.7.2 Measuring extracellular acid phosphatase activity produced by WT and Δ*aph1-1*

C. neoformans strains (WT and *Δaph1-1)* were grown overnight in YPD broth. The cells were washed with water and resuspended in either acid phosphatase suppressing medium (with phosphate); MM-KH_2PO_4 (0.5% KH_2PO_4, 15 mM glucose, 10 mM $MgSO_4.7H_20$, 13 mM glycine, 3.0 uM thiamine) or inducing medium MM-KCl (without phosphate) (see recipe above) at OD600=1. The cultures were incubated at 30°C for 3 hours. Following

incubation, 16 x 50 ul aliquots of each culture were removed and assayed for acid phosphatase production as follows: the cells in each aliquot were pelleted by centrifugation at 14, 000 x *g,* resuspended in 400 μl of 50 mM sodium acetate (pH 5.2) containing 2.5 mM *p*-nitrophenyl phosphate and incubated at 37°C. At 5 min intervals over an 80 min time period, the reaction in a single aliquot of induced and non-induced culture was stopped by adding 800 μL of saturated Na_2CO_3. Cells were again pelleted by centrifugation and the OD of the supernatant was measured spectrophotometrically at 420 nm to determine the extent of pNPP hydrolysis. The pNP hydrolysis product is yellow and absorbs maximally at 405 nm. The assay was performed in duplicate.

2.8 Assessing Aph1 substrate specificity using the Malachite Green Assay

To identify substrates of Aph1, the malachite green assay was performed in a 96 well plate according to the manufacturer's instructions (Cayman chemical). The Malachite Green assay is a quick and reproducible method for measuring free inorganic phosphate in aqueous solutions, including that released by acid phosphatases. The assay is based on the formation of a complex between malachite green molybdate and free orthophosphate that absorbs at 620-640 nm (Cayman chemical).

WT and *Δaph1-1* strains were taken out of glycerol stock, grown overnight on SAB plates at 30°C and inoculated to an OD600 =1 in MM-KCl (low phosphate) medium. The strains were then grown overnight at 30°C with shaking (200 rpm) to allow induction of *APH1* expression in the WT. The cells were centrifuged at maximum speed for 2 min. Each supernatant was collected as the source of enzyme for the assay and a master mix was prepared which contained 250 μl of enzyme (or 250 μl ultra-pure free water to serve as a no-enzyme control), 33.5 μl of 3M sodium acetate (pH 5.2) and 716.5 μl of water. Each reaction contained master mix (25 μl) and 25 μl of 10 mM substrate. The reactions were incubated at 37°C with shaking for 40 min (Figure 3.8A) or for 60 min, with readings taken every 10 min (Figure 3.8B and C). Following incubation for the indicated times, 10 μl of the reaction (containing 2.5 μl of the original enzyme) was combined with 40 μl of water, and 5 μl of MG Acid Solution was added. The tube was mixed by gentle tapping, incubated for 10 min at room temperature and 15 μl of Malachite Green (MG Blue Solution) was then added. Following mixing, the tubes were then incubated for 20 min at room temperature. During

the incubation with MG Blue, each reaction including the 'no enzyme' control was transferred to a 96 well plate. After the incubation the absorbance was determined using a microplate reader at 650nm. The amount of inorganic phosphate produced and hence, the Aph1 substrate preference, was determined using a standard curve which was set up according to the manufacterer's instructions. Each result was corrected by subtracting the absorbance obtained for the no enzyme control which was a measure of the spontaneous breakdown of substrate.

2.9 Adhesion assay

The adherent lung epithelial cell line, A549, was seeded into 24 well plates at a concentration of 1.3 x 10^5 cells/ml/well in RPMI/10% foetal calf serum and incubated overnight at 37˚C in a 5% CO_2 atmosphere. WT and *Δaph1-1* were grown overnight in Aph1 inducing medium (MM-KCl, no phosphate) using inoculum from a freshly grown SAB plate. The fungal cells were washed with water, counted and resuspended at a concentration of 5 x 10^6 cells per well in the 2 day-old (spent) A549 cell culture medium. Spent medium was used instead of fresh medium to ensure that phosphate remained depleted and, hence, that levels of secreted Aph1 remained high during the adhesion assay. Cryptococcal cells were then added to the A549 monolayers and incubation was carried out for 2 h. The media was then aspirated and the monolayer washed 3 times with PBS to remove unbound *C. neoformans* cells. After washing, 0.05% SDS was added to the monolayer to dislodge the cryptococcal cells from the A549 monolayer. At this concentration of SDS, the A549 cells are lysed while the cryptococcal cells remain intact (Voelz *et al.*, 2010). The mixture was then plated out onto SAB plates and the number of colony forming units (CFUs) determined following 2 days incubation at 30°C.

2.10 Survival Studies

2.10.1 *Galleria mellonella* infection model

C. neoformans WT, *Δaph1-1* and *Δaph1-2* cells were grown overnight, pelleted by centrifugation, and resuspended in water at a concentration of 10^8 cells/ml. *G. mellonella* larvae (10 to 20 per strain) were inoculated with 10 μl of cell suspension (10^6 yeast cells) by injection into the hemocoel via the lower pro-legs. The viability of each inoculum was

assessed by performing serial 10-fold dilutions, plating the dilutions onto Sabouraud (SAB) agar plates, and counting the CFU after a 3-day incubation at 30°C. Inoculated larvae were monitored daily for 13 days. The Kaplan-Meier method in the SPSS statistical software program (version 20) was used to estimate the differences in survival (log rank test) and to plot the survival curves. In all cases, a *p* value of less than 0.05 was considered statistically significant.

2.10.2 Murine inhalation model of cryptococcosis.

All procedures described were approved and governed by the Sydney West Local Health District Animal Ethics Committee, Department of Animal Care. Survival analysis was conducted using 7-week-old female BALB/c mice obtained from the Animal Resource Centre, Floreat Park, Western Australia, Australia. The mice were anesthetized using isoflurane (in oxygen) delivered via an isoflurane vaporizer attached to a Stinger small animal anesthetic machine (Advances in Anaesthesia Specialists). Groups of 10 to 20 mice were then inoculated intranasally with *C. neoformans* WT, *Δaph1-1* or the *Δaph1-2* mutant strain ($5x10^5$ yeast cells in 20 µl phosphate-buffered saline [PBS]) and observed daily for signs of ill health. Numbers of viable yeast cells inoculated into the nares were later confirmed by quantitative culture. Mice which had lost 20% of their pre-infection weight, or which showed debilitating clinical signs prior to losing this weight, including hunching, respiratory distress, excessive fur ruffling, or sluggish/unsteady movement, were deemed to have succumbed to the infection and were euthanized by CO_2 inhalation followed by cervical dislocation. Differences in survival were determined with SPSS (version 20) statistical software, using the Kaplan-Meier method (log rank test), where a *p* value less than 0.05 was considered statistically significant.

2.11 Drop Dilution Assays

2.11.1 Cell preparation and dilution

All *C. neoformans* strains were grown overnight in Yeast Extract Peptone Dextrose (YPD) broth (Appendix 2) at 30°C. Following incubation, cells were centrifuged at 4,766 x *g* for 10 min after which the cell pellet was re-suspended in fresh YPD broth. Serial 10-fold dilutions of each strain were prepared with distilled water (10^6-10^1 cells/3µL)

2.11.2 High-Temperature Growth Assay

3 µL of each dilution prepared in 2.12.1 were dropped onto YPD agar and the plates were inverted and incubated at 30°C (control) and 37°C for 72 hours, after which growth was recorded and photographed.

2.11.3 Cell Wall Integrity and high salt stress assay

For the assay 3 µL of each dilution prepared in 2.12.1 was dropped onto YPD agar containing, 1.5 mg/ml Calcofluor White (Fluorescent Brightener 28), 0.8 M NaCl, 0.5% Congo Red or 0.01% SDS (Appendix 2). Except for NaCl, these substances are all cell wall perturbing agents. A YPD agar plate containing no cell wall perturbing agent was used a control. All plates were inverted and incubated at 30°C for 72 hours after which growth was recorded and photographed.

2.12 Capsule Production Assay

2.12.1 Capsule Induction

All *C. neoformans* strains were grown, prepared and serially diluted as in 2.11. Each dilution was dropped onto RPMI-1640 agar (pH 7.0). Plate were inverted and incubated at 37°C within a 5% CO_2 atmosphere (to mimic conditions *in vivo*) for 4 days. Cells were scraped from the plate, counter-stained with India Ink, and capsule production was assessed under a light microscope. Images were then captured at 100x magnification.

2.12.2 Measurement of Capsule Size

The images obtained in Figure 3.12 were viewed using ImageJ 1.45s software. The diameter of the whole cell (including capsule) and cell body was then measured on 40 cells. The average capsule:cell body ratio was calculated using the following formula: diameter of the cell including capsule/diameter of the cell body.

2.13 Determining *APH* mRNA expression levels by semi-quantitative real time PCR (q-PCR)

2.13.1 Inducing *APH* gene expression

WT and *Δaph1-1* were grown overnight in YPD, washed and incubated for 3 hours in inducing (MM-KCl) or suppressing (MM-KH_2PO4) medium and then snap-frozen in liquid nitrogen.

2.13.2 RNA extraction and purity assessment

The cells prepared above were homogenized by bead beating using the mini bead beater (Mini bead beater-8 BIOSPEC PRODUCTS) in the presence of glass beads and TRIZOL® (Ambion) and RNA was extracted and precipitated from the aqueous phase. Briefly, 0.5ml of isopropyl alcohol per 1ml of TRIZOL® reagent was added to precipitate out the RNA. Samples were incubated at RT for 10 min and centrifuged at 12000 x *g* for 10 min at 4°C. Supernatants were removed and the RNA pellets were washed with 1ml 75% ethanol per 1ml of TRIZOL® reagent, followed by centrifugation at 7600 x *g* for 3 min at 4°C. Supernatants were removed and the RNA pellet was air-dried for 5-10 min. Depending on RNA pellet size, the pellets were re-suspended in 40-70µL of UltraPure water. A 1:10 dilution was made with UltraPure water and RNA concentration and purity was determined using a NanoDrop by measuring absorbance at 260nm and 280nm (A260 and A280 respectively). A pure RNA sample was indicated by an A280/A260 ratio of 1.8-2.0.

2.13.3 cDNA Synthesis

Contaminating DNA in the RNA samples prepared in 2.13.2 was removed prior to complementary DNA (cDNA) synthesis as follows. A reaction mixture was prepared in PCR tubes, consisting of 6.0µL RNA sample (containing 2µg total RNA made up to volume with UltraPure water), 2µL MMLV 5x reaction buffer and 2µL DNase RQ1 (Appendix 2). Samples were incubated at 37°C for 30 min in a PCR machine, followed by the addition of 1µL RQ1 DNase stop solution (Appendix 2), after which samples were incubated for a further 10 min at 65°C to inactivate DNase. Oligo dT primer (1 µL) (Appendix 2) was then added and the samples were heated for 5 min at 70°C in the PCR machine. The samples were then placed immediately on ice. The PCR machine was set at 42°C. A master mix containing the following

components was prepared: 3µL MMLV 5x reaction buffer, 5 µL dNTPs 2.5 mM each, 1 µL MMLV-RT and 4 µL UltraPure water per reaction. 13 µL of the master mix was added to each PCR reaction tube. A control reaction was also prepared using UltraPure water as the replacement for MMLV-RT (-RT control). The total reaction volume per sample was 25 µL. Samples were then incubated for 1 hour at 42°C after which they were stored at -80°C until required for qRT-PCR.

2.13.4 Quantitation of APH transcripts in the presence and absence of phosphate

APH transcripts (*APH1*, *APH2*, *APH3* or *APH4*) were quantified by qPCR using cDNA prepared from WT and *Δaph1-1* (as described in 2.13.3) and SYBR Green real time PCR master mix (Life Technologies) on a Rotorgene 6000, 1 Corbett Research qPCR machine.

Table 3. List of primer sequences used for qPCR. (s) indicates sense and (a) antisense

Primer	Sequence
Primers for *qPCR*	
APH1qRT-s	5'-CCTACTTCCCACTCAACCAATCCA-3'
APH1qRT-a	5'- CCTGCGAAGCCACAAACGAA-3'
APH2qRT-s	5'-TCTCGGTCACTCTGCCTTCT-3'
APH2qRT-a	5'-CGCCTTAGCAGGAGCATATC-3'
APH3qRT-s	5'-GACCGATTCTGCTCCTCAAG-3'
APH3qRT-a	5'-GGGACGATTCGGGAAAGA-3'
APH4qRT-s	5'-AAAGCAATGCCACGGTAAAC-3'
APH4qRT-a	5'-CCCAAGCCTGTAGATTGCAT'-3'
ACT1qRT-s	5'- ATGGTATTGCCGAC CGTATG -3'
ACT1qRT-a	5'-CTCTTCGCGATCC ACATCTG-3'

**APH1* expression was calculated using the ΔΔCt method using the housekeeping gene, actin, (*ACT1*), for normalization.

3 Results

3.1 Identification of putative acid phosphatases encoded by the *C. neoformans* genome

To identify putative acid phosphatases encoded by *C. neoformans* genome, a BLAST search of the *C. neoformans* Serotype A strain H99 genomic database (CNAG) (http://www.broadinstitute.org/annotation/genome/cryptococcus_neoformans/MultiHome.html) was performed using the protein sequence of the secreted acid phosphatase, Pho5, of *Saccharomyces cerevisiae* as a query. The search found four putative acid phosphatases: CNAG_06967, CNAG_02681, CNAG_06115 and CNAG_02944, with homology to Pho5. Analysis of the corresponding proteins with the SignalP 4.1 prediction program (http://www.cbs.dtu.dk/services/SignalP/) revealed that only CNAG_02944 is predicted to be secreted, since it contains a secretion signal peptide at the N-terminus (Figure 3.1).

From here on, CNAG_02944 will be referred to as *APH1*. Analysis of the predicted amino acid sequence of Aph1 using pfam (http://www.ncbi.nlm.nih.gov/Structure/cdd/cddsrv.cgi?ascbin=8&maxaln=10&seltype=2&uid=pfam00328) indicates that this protein belongs to branch 2 of the histidine phosphatase superfamily.

MRSAALFALLPILANAAVERRTADSNVGSTTSDVFPPAGTSVNSKLFPAESVVGYPGATVT
GAEPAAAVTAAAYAYNDGTSNSFPLVADQPTGNGSEGFDVFKYWGNLSPWYSVPSSFYGLND
TSPLIPDSCSITQVHLLYRHGARYPTSGAGPSTFAAKLADATAQDGGFTAKGDLDFLNKWTY
KLGAELLTPFGRLQNFELGVTFRQQYGELLNNFTEQGALPVFRTESQDRMVKTAENFAAGFF
GVPEYLDQVSIELMVETSGVNNTGAPYETCPNSNIASRGSLGSTAASSFATDAFNGTVSRLQ
SYINGVEFDTTDVLAMLQLCSYETDALGYSAFCGVFTEEDFKNYEYYFDLNFYYNNGAGSPV
AAAQGKGFLEEFVARFTQTPITSSNSSVNTNLDSNSTYFPLNQSIYADATHEVVLLDTFTAF
NLSALFSTGPLPVDKRAEGSSFVASQVVPFATHMVVQVLECADQTPSKQMRFMINDAVLPLD
KSYEGCGWNKDGMCAFDTVVAALQKRIAEIDYDYDCHGDYTVEAGHDYNGRAPRA

Figure 3.1 Predicted amino acid sequence of Aph1 (CNAG_02944).

The secretion signal peptide is highlighted in yellow. The histidine phosphatase domain is indicated by the blue highlight and was used in the clustering analysis in Figure 3.2.

3.2 Protein clustering analysis

To determine the degree of similarity among cryptococcal acid phosphatases, and between cryptococcal acid phosphatases and those produced by other fungal species, a clustering analysis was performed using the Phylogeny.fr software (http://www.phylogeny.fr/). Due to low sequence similarity among fungal acid phosphatases, only the histidine phosphatase domains (see blue highlight in Figure 3.1) were used in the analysis. The results are shown in Figure 3.2.

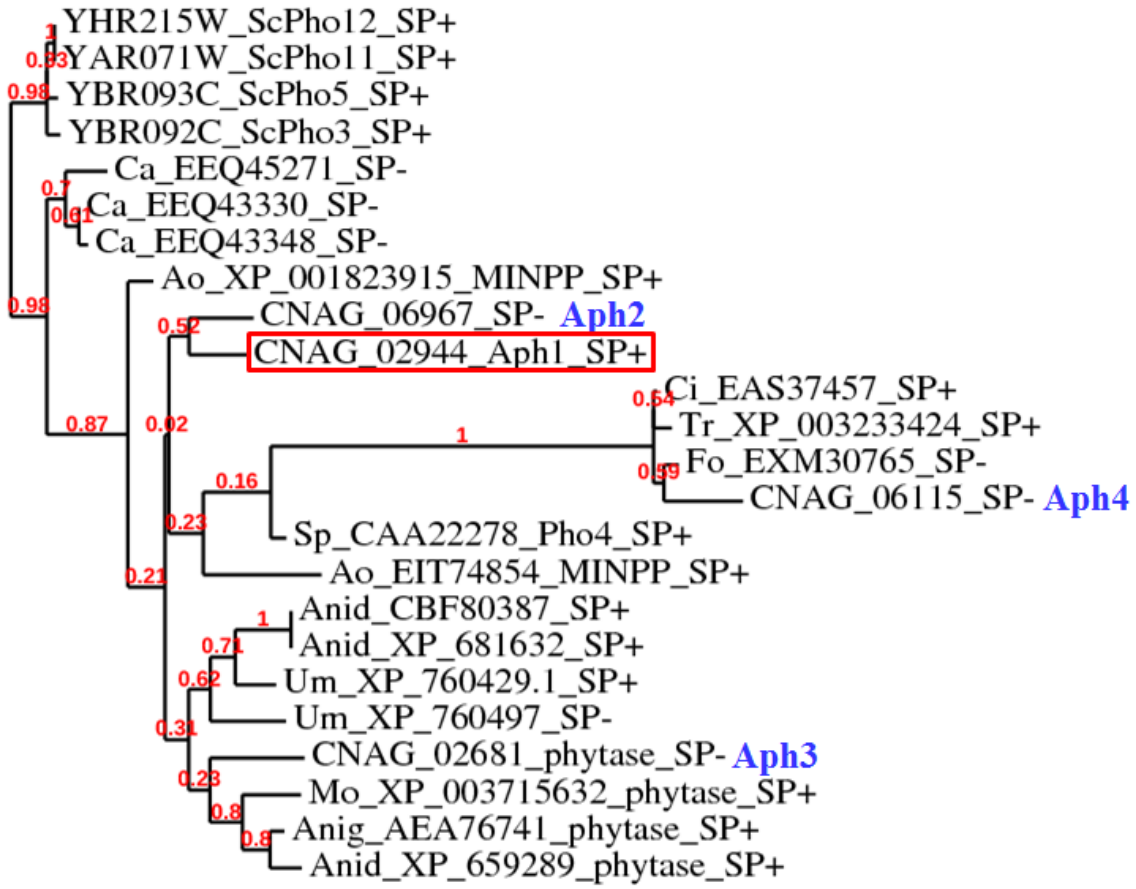

Figure 3.2 Protein clustering analysis based on the alignment of *C. neoformans* acid phosphatases and their homologs in other fungal species.

SP+/- indicates presence or absence of the secretion signal peptide. Only the histidine phosphatase domains were used in this analysis. Unless otherwise indicated, the accession numbers used above are from the NCBI database: Mo, *Magnaporthe oryzae*; Aniger, *Aspergillus niger*; Anid, *Aspergillus nidulans*; Sp, *Schizosaccharomyces pombe*; Ao, *Aspergillus oryzae*; Um, *Ustilago maydis*; Fo, *Fusarium oxysporum*; Tr, *Trichophyton rubrum*;

Ci, *Coccidioides immitis*; Ca, *Candida albicans*; CNAG, *Cryptococcus neoformans* serotype A genome (gene IDs from the Broad Institute database), Sc; *Saccharomyces cerevisiae* (gene IDs from the SGD database). SP+/- indicates presence or absence of the secretion signal peptide. Only the histidine phosphatase domains were used in this analysis. Bootstrap values, which are a measure of the confidence of the branching prediction, are shown in red. The position of cryptococcal Aph1 is highlighted by the red frame.

Table 4. Percentage similarity and identity of the four acid phosphatases encoded in *C. neoformans* genome respective to each other. Predicted protein sequences were used to determine the respective percentages.

CnAPH	APH1		APH2		APH3		APH4	
	Identity	Similarity	Identity	Similarity	Identity	Similarity	Identity	Similarity
APH1			40.3%	59.5%	24.2%	43.2%	19.5%	32.2%
APH2	40.3%	59.5%			25.6%	41.2%	22.1%	34.3%
APH3	24.2%	43.2%	25.6%	41.2%			17.8%	31.0%
APH4	19.5%	32.2%	22.1%	34.3%	17.8%	31.0%		

Clustering analysis indicates that the closest homolog of Aph1 (40.3% identical and 59.5% similar) is CNAG_06967 (*APH2*), which is not predicted to be secreted. Both proteins are close to phytases (phytic acid-degrading enzymes), MINPP (multiple inositol polyphosphate phosphatases) from *Aspergillus oryzae* and Pho4 from *Schizosaccharomyces pombe*, but not to Pho3/5/11/12 from *Saccharomyces cerevisiae*. Interestingly, the predicted phytase, CNAG_02681 *(APH3)*, clusters with the rest of the phytases from other fungal species, while CNAG_06115 *(APH4)* is the most distantly related to other acid phosphatases used in the analysis. Both secreted and intracellular acid phosphatases are represented in fungi. For example, all acid phosphatases of *S. cerevisiae* are secreted, while their counterparts in human pathogen *Candida albicans* are intracellular. Similar to *C. neoformans*, the genome of another basidiomycete, *Ustilago maydis*, contains both secreted and intracellular acid phosphatases.

3.3 Characterization of Aph1 using targeted gene deletion analysis

***APH1* gene deletion**: To determine whether Aph1 contributes to the extracellular acid phosphatase activity produced by *C. neoformans*, and to assess its role in cryptococcal cellular function, phosphate homeostasis and virulence, the *APH1* gene (CNAG_02944) was selectively deleted in *C. neoformans* strain H99 (wild type, WT) as described in section 2.6. An *APH1* gene deletion construct, containing an antibiotic resistance marker, was created *in vitro* by overlap PCR and introduced into WT *C. neoformans* using biolistic transformation (Figure 3.3). Biolistic DNA delivery, as opposed to heat shock or electroporation, is essential to allow the DNA to penetrate the capsule and cell wall. Once inside the nucleus, the deletion construct can undergo homologous recombination with the genomic DNA flanking *APH1*, thus replacing the *APH1* coding sequence with the resistance marker (Figure 3.3).

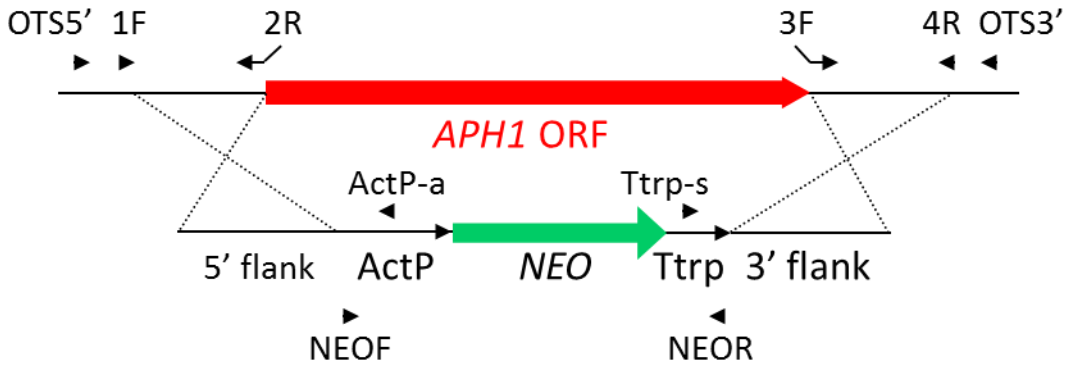

Figure 3.3 Diagram of the *APH1* gene deletion construct (bottom) and the position of its integration site in the genome (top). Note: Figure not to scale.

The deletion construct consisting of the neomycin/G418 resistance marker (NEO) regulated by the actin promoter (ActP) and Tryptophan terminator (Ttrp) and the 5' and 3' flanking regions of the *APH1* gene, was created *in vitro* by overlap PCR and introduced into *C. neoformans* by biolistic transformation. Stable G418-resistant recombinants created by homologous integration of the deletion construct at the native *APH1* gene locus were selected on G418 agar plates. Arrows and arrowheads indicate the primer binding sites and the dotted lines represent homologous recombination. All primer sequences indicated are listed in Section 2.6.2, Table 2. ORF is open reading frame.

In fungal cells, neomycin resistance cassette provides resistance to the related antibiotic, geneticin (G418). Geneticin-resistant transformants were selected by growth on G418-containing plates. 96 transformants were then subjected to a preliminary screen to identify those that had lost extracellular acid phosphatase activity as a result of successful *APH1* gene deletion. For this screening, each transformant was grown in a single well of a 96 well plate, and was supplemented with the chromogenic acid phosphatase substrate, para-nitrophenolphosphate (pNPP), as described in section 2.7.1. Production of a yellow colour following addition of sodium carbonate was indicative of pNPP hydrolysis by the transformant and the presence of extracellular acid phosphatase activity. Out of the 96 transformants screened, 3 did not produce a yellow colour (i.e. the media remained clear) and thus did not release active acid phosphatase into the medium (Figure 3.4).

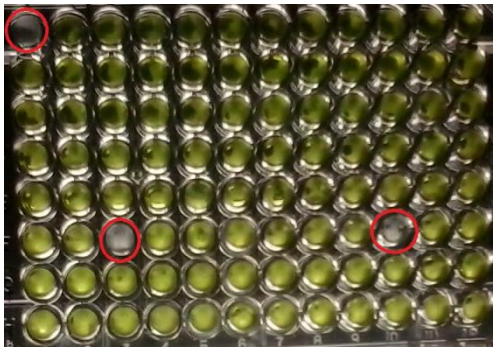

Figure 3.4 Screening of neomycin-resistant transformants for the production of extracellular acid phosphatase activity to identify potential Δ*aph1* mutants.

Each colony was inoculated into phosphate-deficient medium, grown overnight, and then incubated with the chromogenic substrate, pNPP, at acidic pH for 20 min at 37°C. The reactions were stopped by addition of saturated Na_2CO_3. Yellow colour indicates the production of extracellular acid phosphatase activity. Three out of 96 transformants did not produce acid phosphatase activity (media remained clear) and are indicated by red circles.

Genomic DNA was then prepared from these 3 transformants (named #1, #2 and #3) as described in section 2.5 and PCR was performed to confirm that integration of the deletion construct had occurred at the *APH1* gene locus (Sections 2.3 and 2.6). PCR primer sets OTS5'/ActP-a and Ttrp-s/OTS3' were designed to amplify the DNA spanning the 5' and the 3' integration sites, respectively (Figure 3.3), giving product sizes of 787bp and 952bp, respectively. The results in Figure 3.5 show that the expected PCR products were present in

clones #2 and #3, but not in clone #1, confirming that targeted *APH1* deletion had occurred in clones #2 and #3 only. A faint band of the correct size was obtained for the PCR of the 3' flanking region of clone #1, which is most likely to be contamination from the adjacent lane, and no band was obtained for the PCR of the 5' flank. As expected, no bands were visible in the control PCR where WT was used as a template.

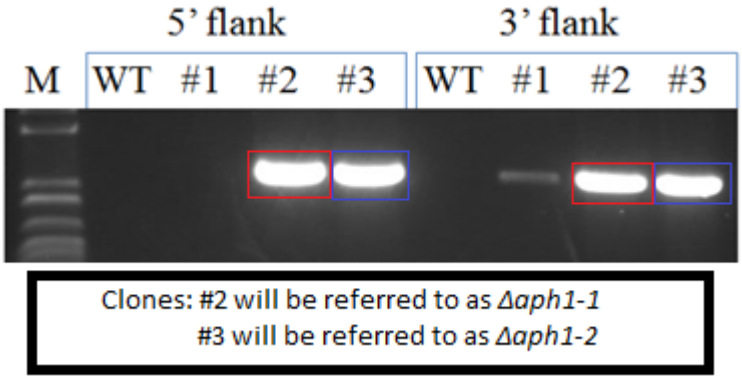

Figure 3.5. PCR verification of *APH1* gene deletion in transformants with defective acid phosphatase secretion.

Genomic DNA was extracted from those transformants that did not secrete active acid phosphatase (clones #1 , #2 and #3 in Figure 3.4) and used as a template in PCR with primers APH1-OTS5'/ActP-a and Trp-s/APH1-OTS3'(see Figure 3.3 and Table 2.)**.** Only clones #2 (which will now be referred to as *Δaph1-1*) and #3 (which will now be referred to as *Δaph1-2)* had integrated the deletion cassette at the site of the native *APH1* locus, as indicated by the presence of 2 PCR products of the expected size. These bands were absent in the control PCR reaction where WT was used as a template.

3.4 Comparing the production of extracellular acid phosphatase activity by WT and *Δaph1-1* in low and high phosphate

In the model yeast *S. cerevisiae* and in filamentous fungi, a subset of acid phosphatases are secreted in response to a low phosphate environment. These extracellular acid phosphatases then hydrolyse complex organic phosphate sources to release free phosphate (Pi) for uptake via a set of membrane transporters (Figure 1.3).

To confirm that Aph1 secretion is regulated by phosphate availability, *C. neoformans* WT and *Δaph1-1* were incubated in phosphate-deficient (inducing) and phosphate-replete (non-inducing) media for 3 hours prior to the addition of the

chromogenic substrate, pNPP. Hydrolysis of pNPP by extracellular Aph1 was then measured at 5 min intervals over an 80 min time course by taking absorbance readings at 420 nm, the wavelength at which the pNP hydrolysis product absorbs maximally. Figure 3.6 demonstrates that extracellular acid phosphatase activity is only produced by the WT strain in the absence of phosphate. The amount of pNPP hydrolysed by the WT strain increases over the time course and reaches plateau at around 40 min. No acid phosphatase was secreted by *Δaph1-1* in either phosphate deficient or phosphate replete conditions. These findings indicate that almost all of the secreted acid phosphatase activity in strain H99 is contributed by Aph1 and that similar to Pho5 in *S. cerevisiae*, Aph1 secretion in *C. neoformans* is regulated by phosphate availability.

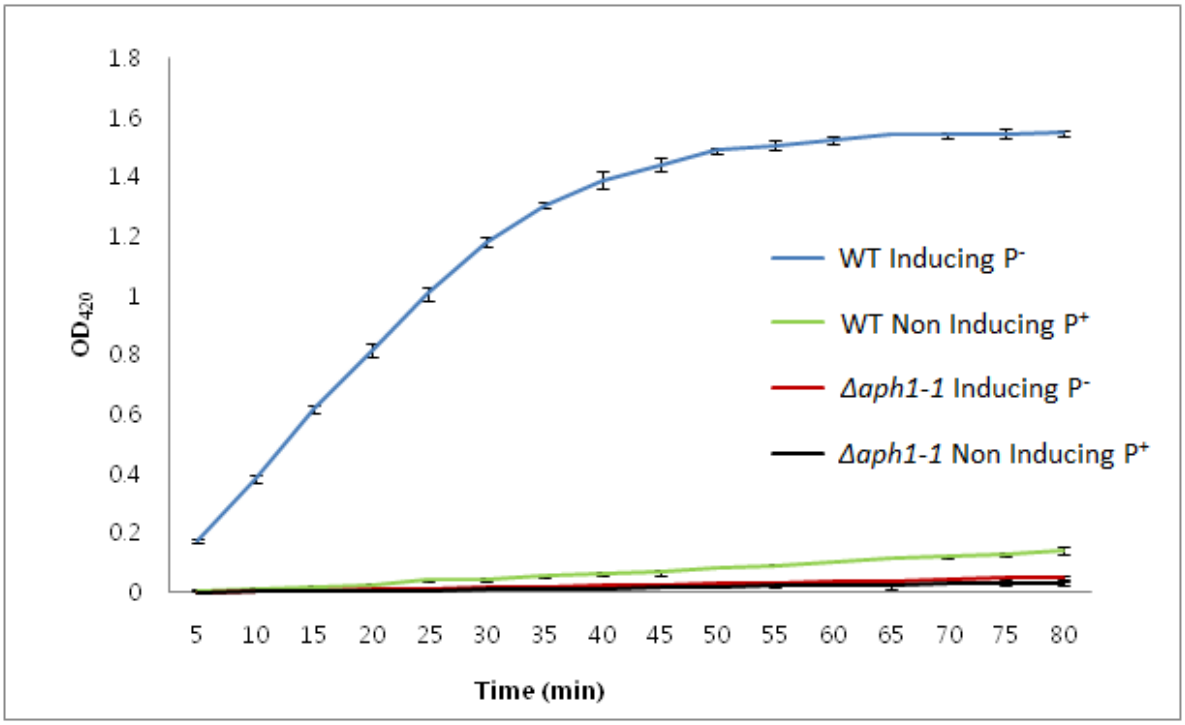

Figure 3.6 Secreted Aph1 activity assay in WT and *Δaph1-1* under inducing (P^-) and non-inducing (P^+) conditions.

WT and *Δaph1-1* were incubated for 3 hours under phosphate replete (MM-KH_2PO_4: non-inducing/P^+) or phosphate-deficient (MM-KCl: inducing/P^-) conditions. The chromogenic acid phosphatase substrate, pNPP, was then added to the medium. Hydrolysis of pNPP by extracellular acid phosphatase(s) was measured at 5 min intervals over an 80 min time course by taking absorbance readings at 420 nm. The results represent the mean and standard error of two biological replicates.

3.5 Comparing *APH1* gene expression in WT and *Δaph1-1* in low and high phosphate using semi-quantitative real time PCR (qPCR)

In S. cerevisiae and filamentous fungi, limited phosphate availability causes acid phosphatase-encoding genes to be transcribed and translated into protein, which is released into the external environment via the secretory pathway. The results in Figure 3.6 demonstrate that secretion of Aph1 is also phosphate-regulated. In order to determine whether Aph1 secretion correlates with *APH1* gene expression, the latter was compared in WT and *Δaph1-1* under inducing and suppressing conditions using qPCR. The results in Figure 3.7 demonstrate that expression of *APH1* in WT was suppressed in the presence of phosphate and induced ~340 fold when phosphate was depleted. As expected, *APH1* mRNA production was absent in *Δaph1-1* under both conditions, confirming that *APH1* had been deleted.

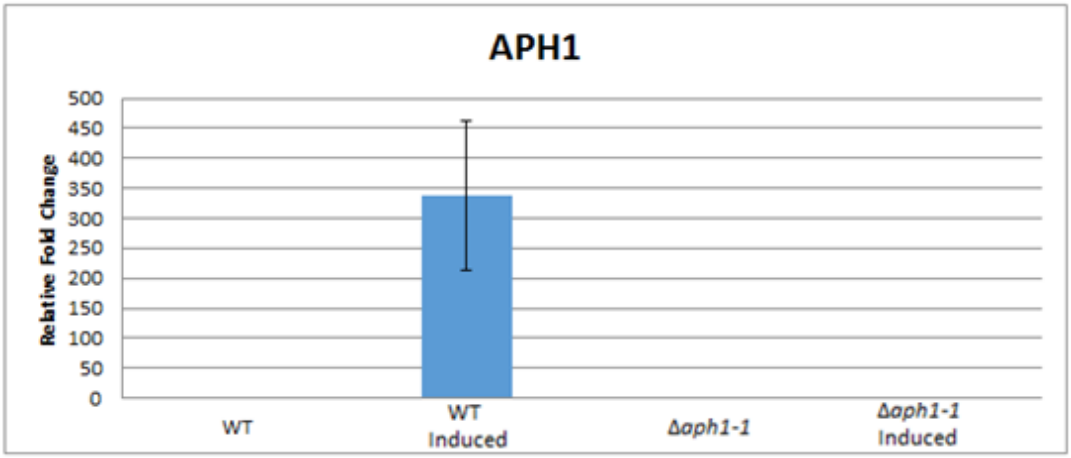

Figure 3.7 Comparing *APH1* gene expression in WT and *Δaph1* in low and high phosphate conditions.

WT and *Δaph1-1* were incubated for 3 hours under phosphate-replete (non-inducing) or phosphate-deficient (inducing) conditions, as in Figure 3.6. RNA was extracted and cDNA synthesized. *APH1* transcripts were quantified by qPCR using the ΔΔCt calculation method after normalizing against expression of the housekeeping gene actin 1 (*ACT1*). The results represent the mean and standard error of 3 biological replicates. The level of *APH1* expression in the induced WT sample was statistically greater than all other samples ($p<0.05$).

3.6 Determining the substrate specificity of Aph1 using a Malachite Green Assay

To identify potential physiological substrates of Aph1, WT and *Δaph1-1* were grown under phosphate-deficient conditions to induce expression of *APH1* and secretion of the Aph1 protein, as shown in Figures 3.6 and 3.7, respectively. The ability of culture supernatants from induced and non-induced cells to hydrolyze a diverse range of phosphorylated macromolecules (amino acids, sugars, nucleotides and lipids) was then compared. The phosphate released from each substrate as a result of Aph1-mediated hydrolysis was quantified spectrophotometrically using a malachite green assay described in 2.8 and the results are shown in Figure 3.8. Culture supernatant from WT, but not from *Δaph1,* readily hydrolyzed the phosphate from the amino acid phosphotyrosine but not from phosphothreonine or phosphoserine (Figure 3.8A). The phosphorylated sugars, glucose-1-phosphate and mannose-6-phosphate, the phosphorylated polyol, β-glycerol phosphate, and the nucleotides, adenosine monophosphate (AMP) and adenosine triphosphate (ATP) were also found to be good substrates of Aph1 (Figure 3.8A). Since Aph1 clusters with phytases produced by other fungal species, IP_6 was also tested as a substrate. However, I was unable to demonstrate that IP_6 was a substrate of Aph1 because the malachite green compound reacted with IP_6 forming a precipitate. The hydrolysis of two of the preferred substrates of Aph1, β-glycerol phosphate (Figure 3.8B) and phosphotyrosine (Figure 3.8C) was also measured over a 60 min time course using the malachite green assay. For both substrates, a linear increase in phosphate release by WT supernatants, but not by *Δaph1-1* supernatants, was observed.

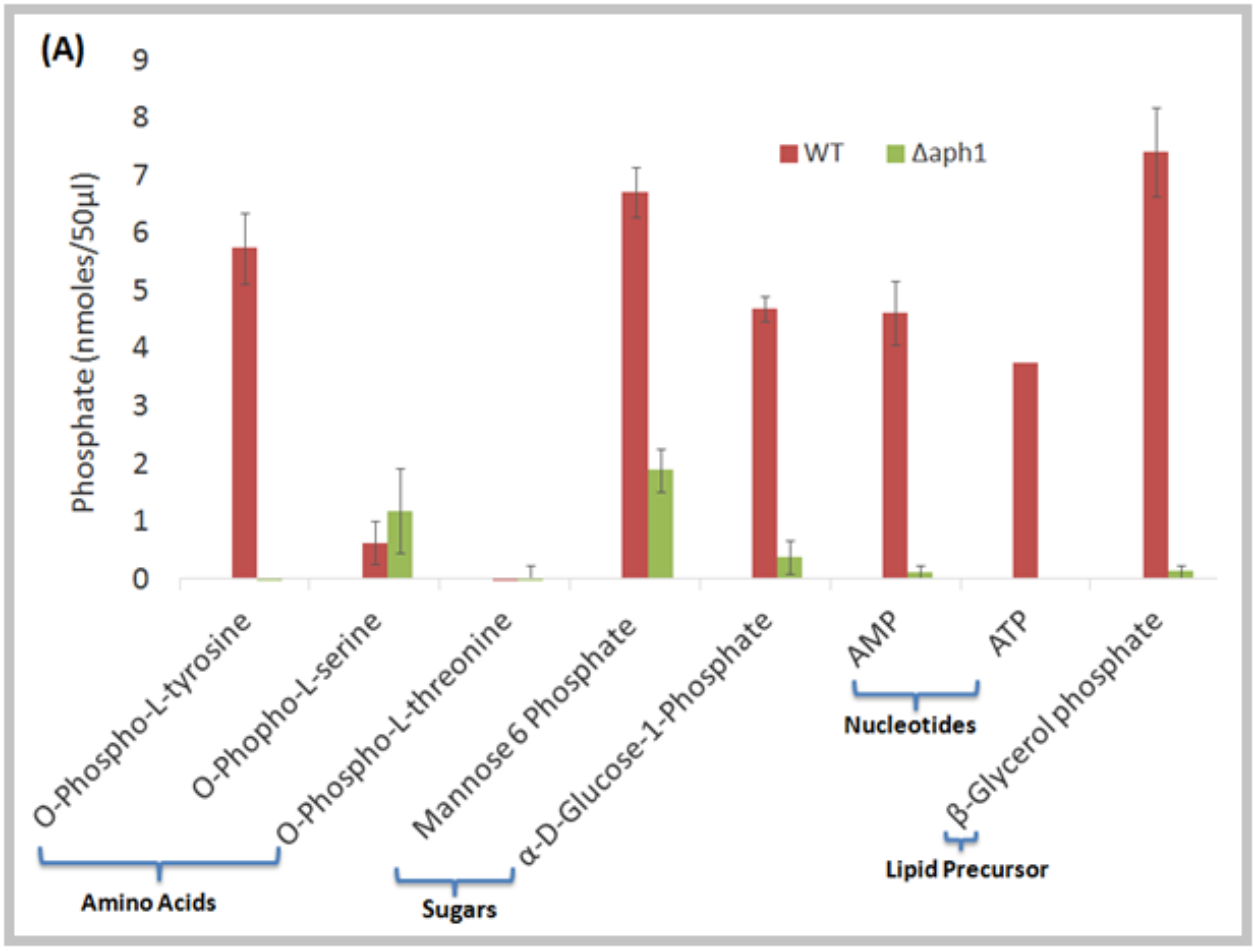

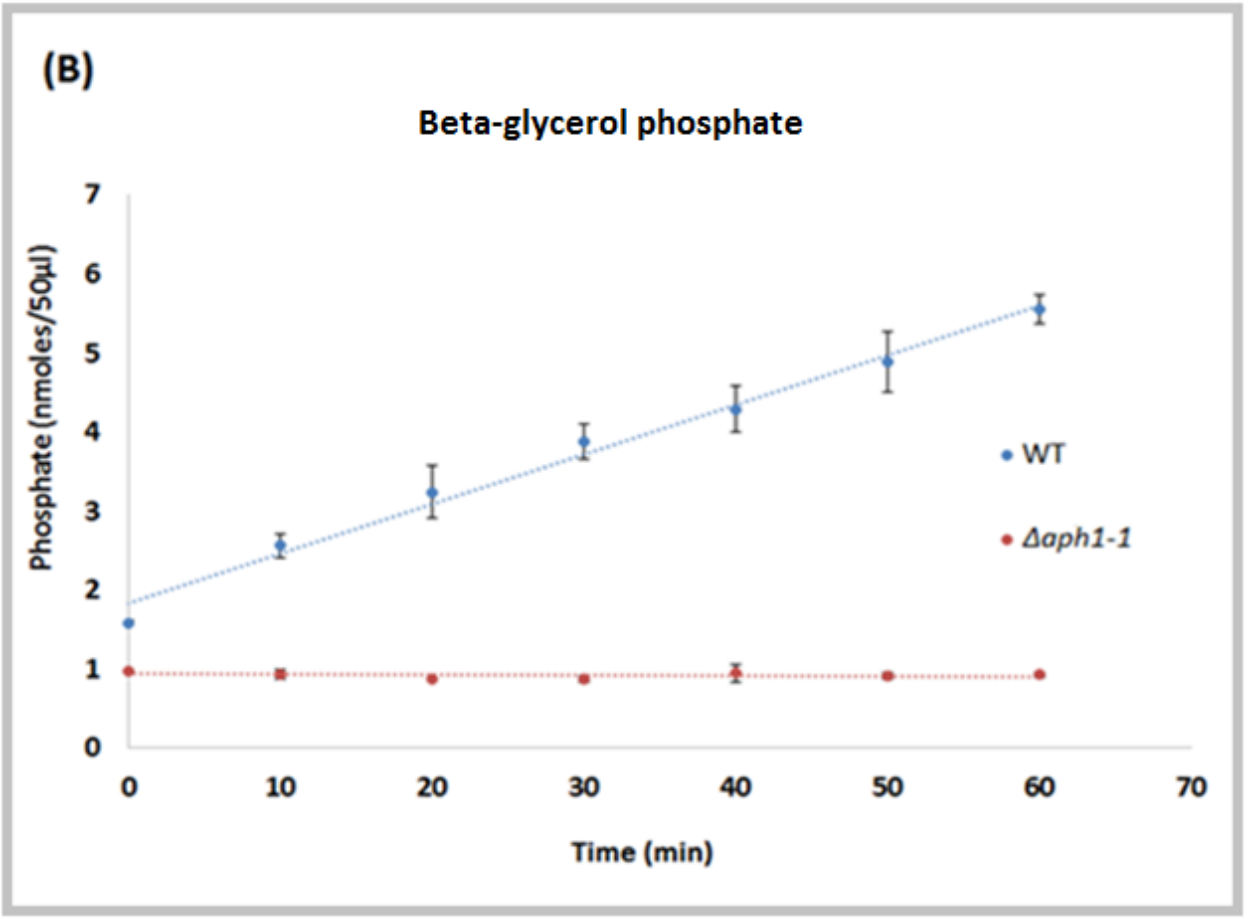

Continued on page 47

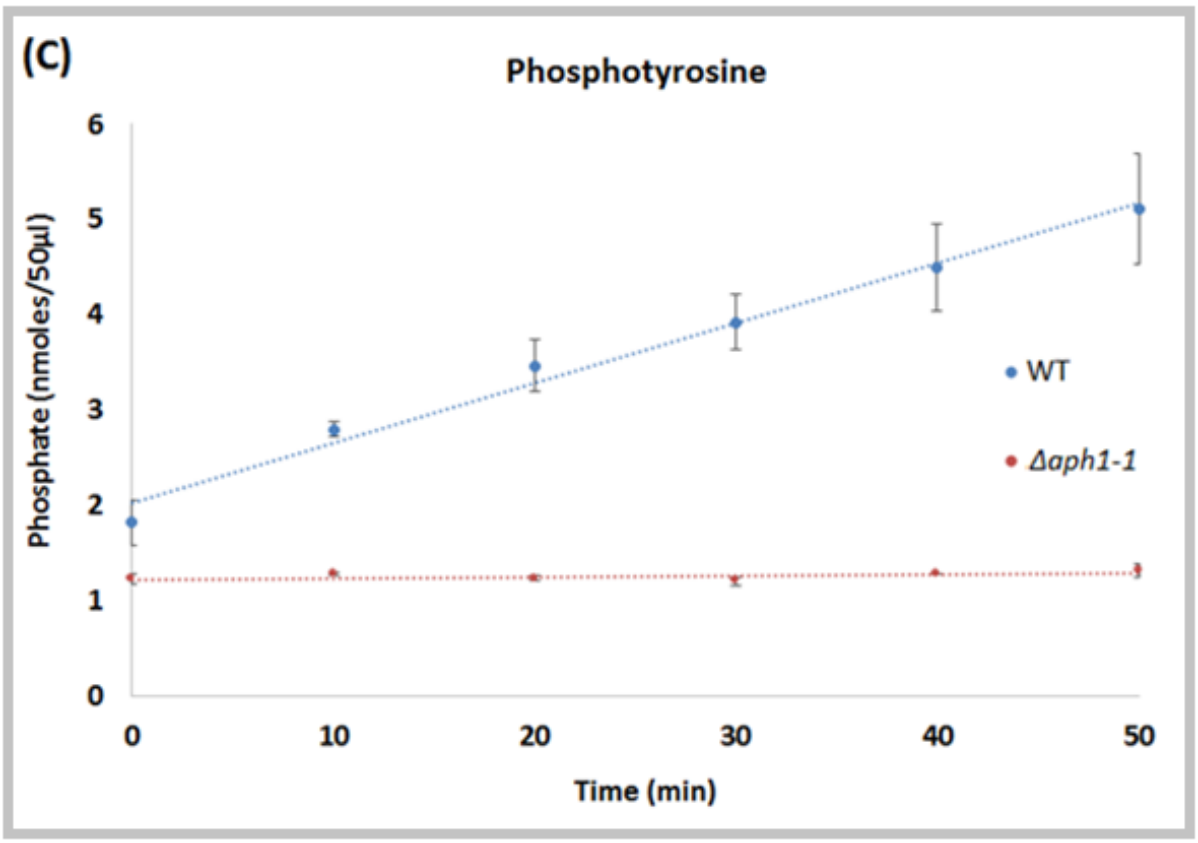

Figure 3.8 Aph1 catalyses hydrolysis of β-glycerol phosphate, glucose-1-phosphate, mannose-6-phosphate, phosphotyrosine, AMP and ATP.

WT and *Δaph1-1* were grown in low phosphate medium overnight to induce *APH1* expression and Aph1 secretion. Secretions were collected as a source of secreted Aph1 enzyme and incubated with the substrates indicated. The amount of free phosphate released from each substrate in 40 min (A) or from two preferred substrates, β-glycerol phosphate (B) and phosphotyrosine (C) over a 60 min time course was then quantified using the malachite green assay as described in 2.8. Except for ATP (one replicate), all experiments were conducted on three biological replicates and error bars indicate standard error of the mean.

3.7 Impact of *APH1* deficiency on fungal growth

3.7.1 Impact of *APH1* deficiency on fungal growth at elevated temperature and in the presence of salt and cell wall perturbing agents

The impact of *APH1* deficiency on fungal growth at elevated temperature, and in the presence of cell wall perturbing agents and high salt concentration was assessed using a drop dilution assay (Figure. 3.9). Cell wall stress resistance was tested since extracellular Aph1 may play a role in modulating the activity of cell wall proteins via their dephosphorylation. The cryptoccocal cell wall is mainly made up of β-(1,3)-D-glucans, β-(1,4)-D-glucans, β-(1,6)-D-glucans, chitin and glycoproteins, which are involved in its synthesis (reviewed in (Doering, 2009)). Congo Red binds to the β-(1,3)-D-glucan chains. Calcofluor white (CFW) binds to chitin and SDS is a detergent which denatures proteins in the cell wall. Under all of these conditions the phosphate levels were sufficient to support growth. *Δaph1-1* grew at a similar rate to WT at 30°C, 37°C and 39°C and in the presence of salt (1M NaCl) and cell wall perturbing agents Congo red, SDS and CFW. *Δaph1-1* also grew at a similar rate to the WT in the absence of free phosphate (0.5% KCl). The growth test was also performed on 0.4% KH_2PO_4 as a phosphate-replete control and, as expected, the growth rate of all strains was similar. Growth in the presence of phytic acid (IP_6) as the sole source of phosphate was also tested since Aph1 showed close homology to many fungal phytases (Figure 3.2). However, the results showed that there was no differences in the growth rate of *Δaph1-1, Δaph1-2* and WT on IP_6.

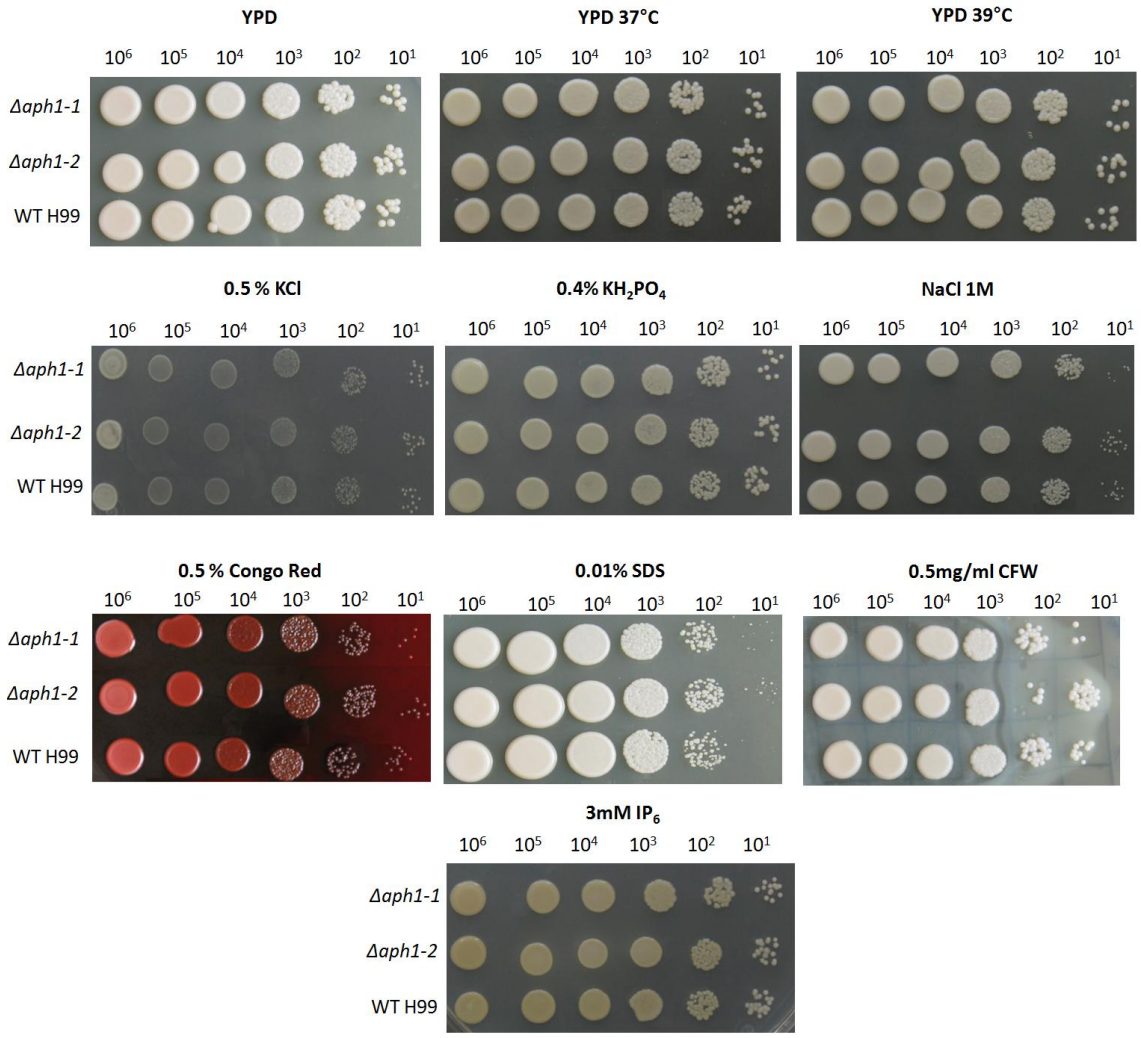

Figure 3.9 Comparison of WT, *Δaph1-1* and *Δaph1-2* growth using a drop dilution assay under the conditions indicated.

Drops containing the indicated number of cells were plated on the different media and incubated for 3 days. Phosphate replete conditions (0.4% KH_2PO_4: non Aph1-inducing), phosphate-deficient conditions (0.5% KCl: Aph1 inducing). Plates containing just YPD, or YPD with NaCl or Congo red or SDS or calcofluor white (CFW), all contained a sufficient source of phosphate. Where IP_6 was used, it was the sole source of extracellular phosphate.

3.7.2 Impact of *APH1* deficiency on fungal growth during multiple stresses

Since *C. neoformans* experiences multiple stresses when infecting a host, including a deficiency in free Pi (Kretschmer *et al.*, 2014), the growth rate of *Δaph1* was compared to WT during Pi deprivation combined with one or two additional stresses: high temperature, salt or cell wall stress (Congo Red). Cells were also starved of phosphate for 3 hours before they were dropped onto phosphate-deficient plates to deplete intracellular polyphosphate stores. However, no differences between the WT and *Δaph1-1* growth rates were observed in any condition (Figure 3.10).

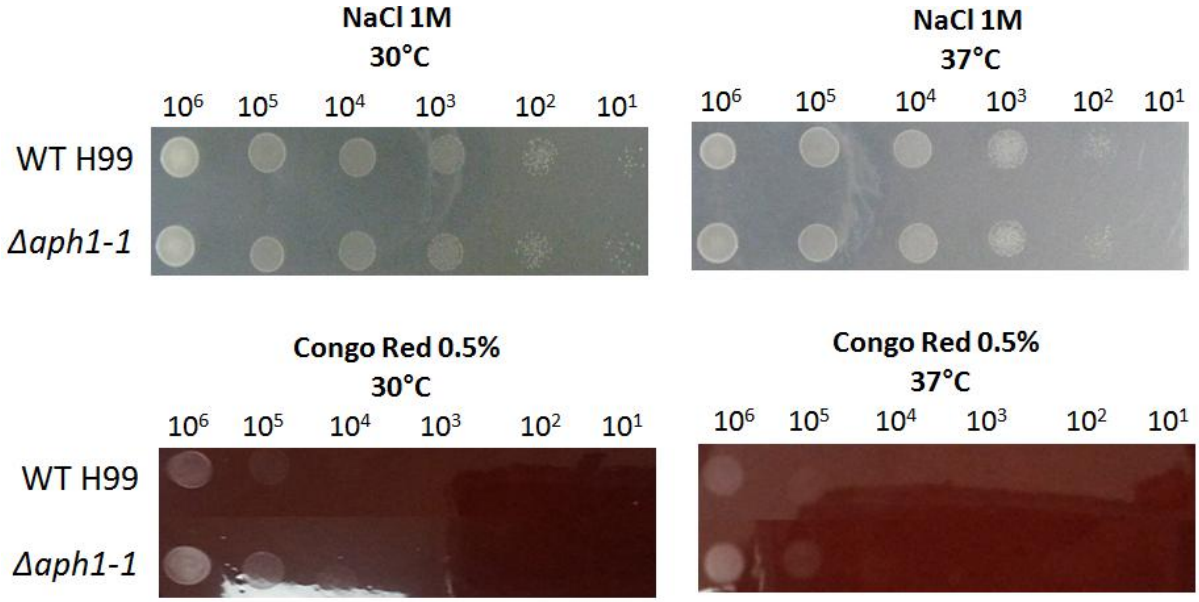

Figure 3.10 Comparison of WT and *Δaph1-1* growth using a drop dilution assay under the conditions indicated.

Cells were grown in Pi-free media for 3 hours prior to plating, to deplete internal stores of polyphosphates**.** Drops containing the indicated number of cells were plated onto plates without phosphate (0.5% KCl: Aph1 inducing) and containing either Congo Red or NaCl. Plates were incubated at either 30°C or 37°C for 3 days.

3.7.3 Impact of *APH1* deficiency on fungal growth in the presence of Aph1 substrates as the sole phosphate source

Growth of WT, *Δaph1-1* and *Δaph1-2* were compared in the presence of β-glycerol-phosphate or glucose-1-phosphate as the sole source of phosphate in a drop dilution assay. β-glycerol phosphate and glucose-1-phosphate are both substrates of Aph1 (Figure 3.8). Control plates containing abundant free phosphate and either glycerol or glucose were also

employed. However, no differences in growth between the WT and the two *Δaph1* strains were observed under any condition tested (Figure 3.11).

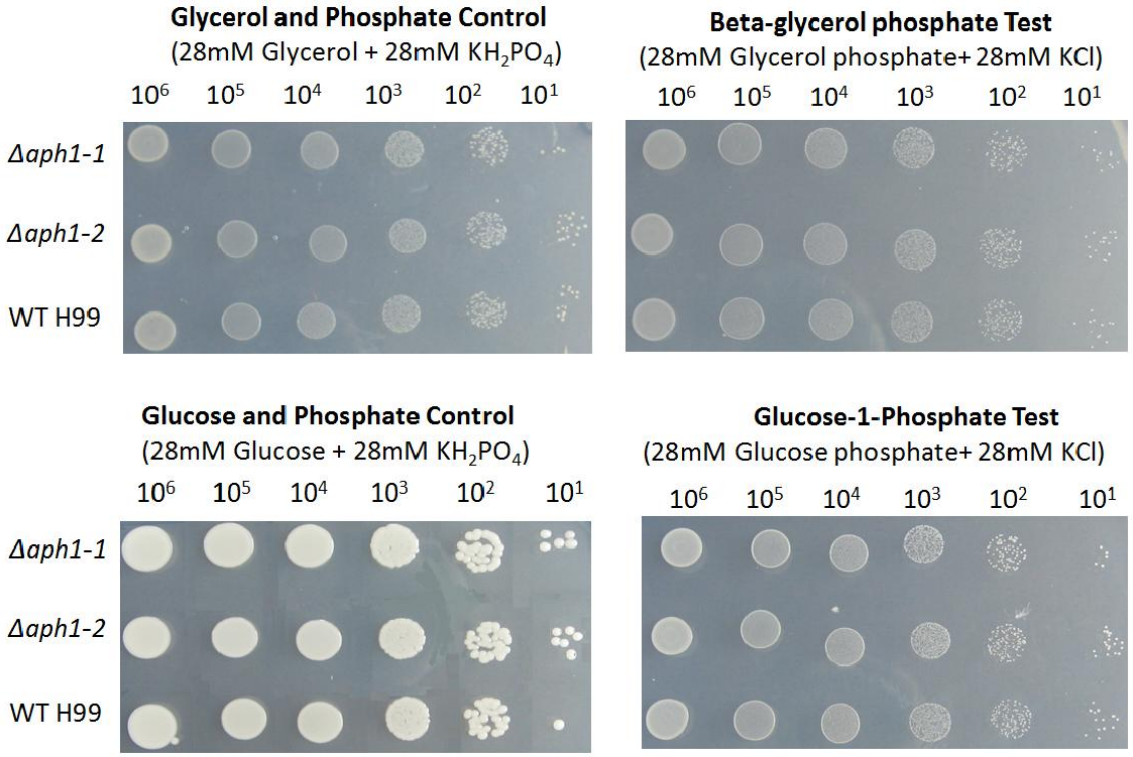

Figure 3.11 Comparison of WT, *Δaph1-1* and *Δaph1-2* growth using a drop dilution assay under the conditions indicated.

Drops containing the indicated number of cells were plated onto control plates: phosphate replete/0.4% KH_2PO_4/non Aph1-inducing containing either free glycerol or free glucose, or test plates: phosphate-deficient/0.5% KCl/Aph1 inducing) containing β-glycerol-phosphate or glucose-1-phosphate as the sole source of phosphate. The plates were then incubated at 30°C for 3 days. β-glycerol-phosphate and glucose-1-phosphate are both substrates of Aph1 (Figure 3.8).

3.8 Impact of *APH1* deficiency on capsule production.

Capsule is a major virulence factor of *C. neoformans* and is anchored to the cell wall. Aph1 protein therefore potentially associates with the capsule during its release from the cells and may play a role in its production. Capsule production was therefore compared in WT (H99) and *Δaph1-1* and using India Ink negative staining and light microscopy as described in 2.12 (Figure 3.12). The size of the capsule was then measured in 40 cells form each strain and expressed relative to the size of the cell body as described in 2.15.2.

However, no statistically-significant difference in the mean capsule: cell body ratio was observed: WT - 1.6±0.394 and *Δaph1*- 1.8±0.126 (p>0.05), with errors representing standard deviation.

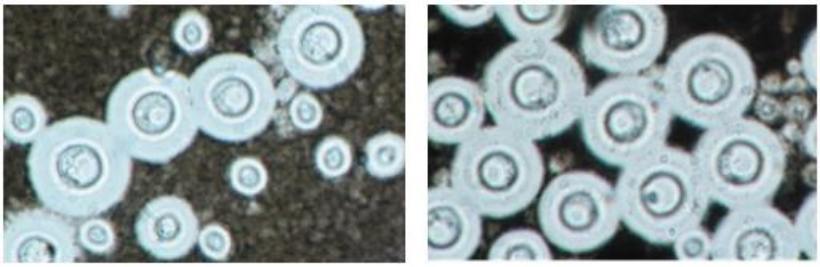

Figure 3.12 Visualisation of the WT and *Δaph1-1* capsules by negative staining with India Ink and light microscopy at 100x magnification.

3.9 Assessing the role of Aph1 in virulence

3.9.1 *Galleria mellonella* model

The contribution of Aph1 to the virulence of *C. neoformans* was investigated in a survival study using two well accepted animal models of cryptococcosis: the greater wax moth, *Galleria mellonella*, and mice (*Mus Musculus*). *Galleria mellonella* larvae were inoculated directly into the haemocoel via injection of Cryptococci into the proleg, while mice were inoculated by inhalation of Cryptococci to mimic the natural route of infection. To determine whether a similar number of viable WT and *Δaph1* cells were inoculated (cell counts determined by microscopy) each inoculum was plated onto agar and the number of CFUs determined after 2-3 days growth at 30°C. The numbers of CFUs obtained for WT, *Δaph1-1* and *Δaph1-2* were within 5% of the microscopy cell counts and within 10% of each other.

The results of the wax moth survival study, where the virulence of WT is compared to *Δaph1-1* and *Δaph1-2,* is presented in Figure 3.13. Five infection groups were created and observed: uninjected larvae, mock (PBS-injected), WT-infected and *Δaph1-1*-infected and *Δaph1-2*-infected. Each group contained 10 larvae except for the *Δaph1-1*-infected group, which contained 20 larvae. No larvae died in the uninjected group while 2 died in the mock-infected group, most likely from physical trauma due to the injection procedure. The median survival time of WT-, *Δaph1-1*- and *Δaph1-2*-infected larvae was 3, 6 and 5 days, respectively.

However, only the median survival of *Δaph1-1*-infected larvae differed significantly from that of WT (P-0.028) (Table 5). This was most likely because more larvae were used.

Table 5. Median survival day of mice infected with *WT, Δaph1-1* and *Δaph1-2.* P-values are also shown.

	Median survival (days)	*p*- value (compared to WT)
WT H99	**3**	
Δaph1-1(n=20)	**6**	**0.028**
Δaph1-2(n=10)	**5**	**0.062**

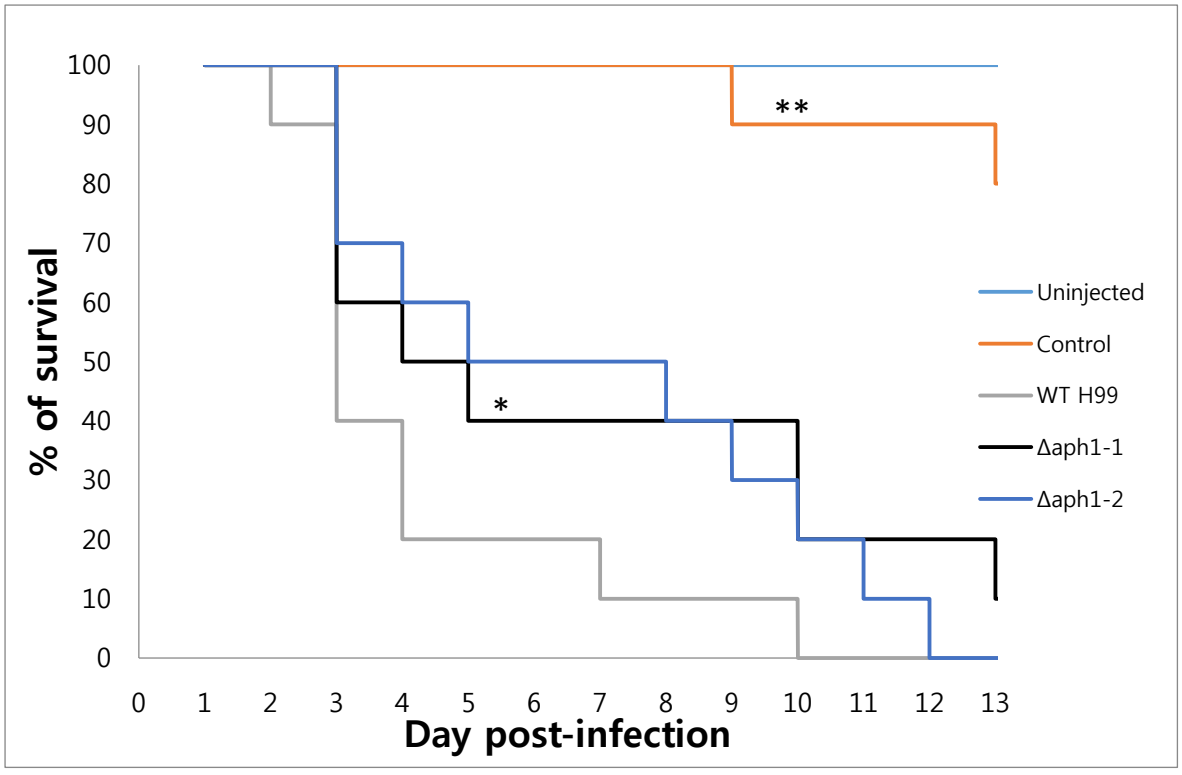

Figure 3.13 Survival study in *Galleria mellonella.*

Larvae were injected with 1 x 10^6 fungal cells via the proleg and their viability was assessed on a daily basis for 13 days. The graph indicates that the WT-infected larvae (grey line) had a lower survival rate compared to *Δaph1-1* (black line) and *Δaph1-2* (thick light blue line) infected larvae. However using a Kaplan Meier log rank test, the difference was only statistical significant when compared with *Δaph1-1* (p-0.028*) where more larvae were used. All of the uninjected larvae and 80% of the PBS-injected controls survived until the

experiment was terminated (day 13). ** indicates statistical significance between the un-injected and PBS-injected controls and both the WT and *APH1* mutants.

3.9.2 Murine model of infection

Galleria mellonella was used as an initial screening tool to test for virulence prior to using mice. As statistical significance was achieved using 20 larvae for the *Δaph1-1* infection group and 10 larvae for the WT infection group, similar numbers of mice were used in the murine survival study. Mice were inoculated intranasally as indicated in 2.10.2 and their health was monitored over a period of 20 days. Mice showing debilitating symptoms of infection were culled and their deaths recorded. Differences in median survival were calculated using a Kaplan Meier log rank test, but the difference in median survival of WT-inoculated larvae (14 days) and *Δaph1-1*-inoculated larvae (17 days) was not statistically significant (p=0.163) (Figure 3.14). However, when a log rank test stratified by species was performed using the WT and *Δaph1-1* data from the larval and mouse study, this combined analysis did demonstrate a statistically significant difference in virulence of WT and *Δaph1-1* (P=0.012) (Figure 3.15).

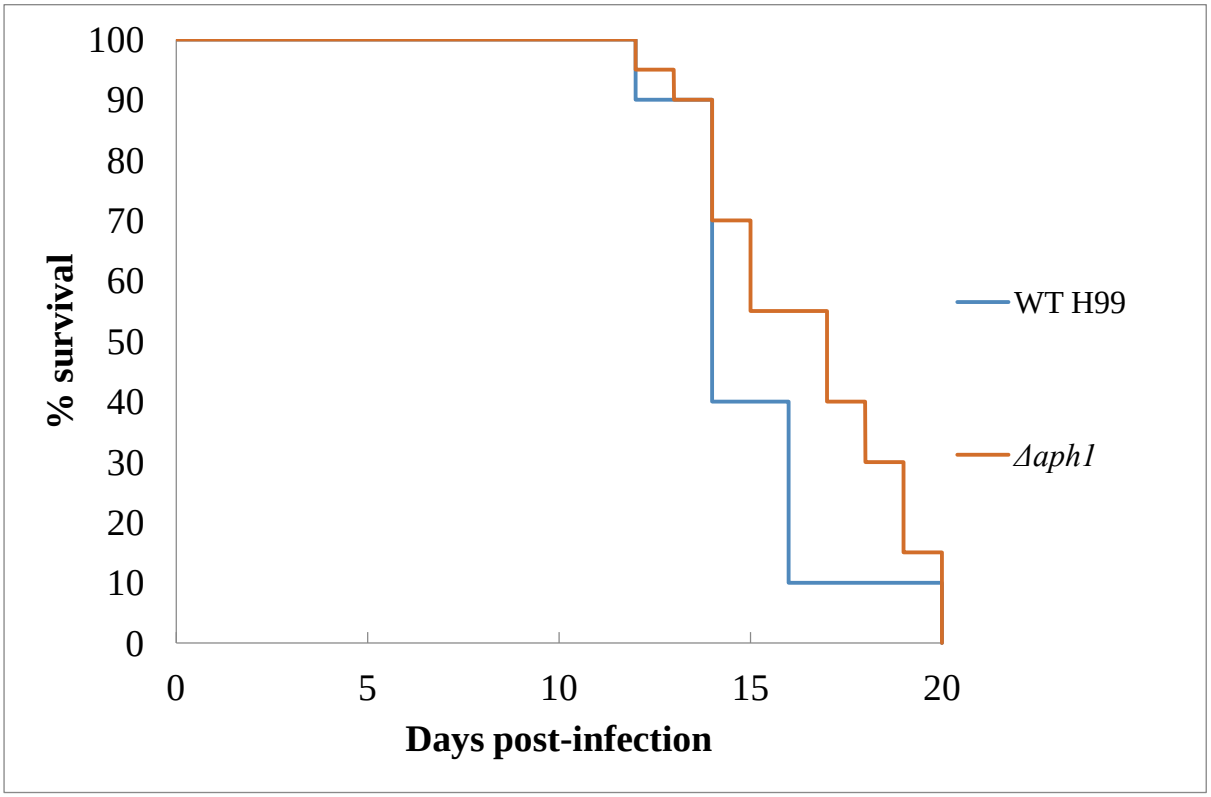

Figure 3.14 Survival study in mice.

The role of Aph1 in fungal virulence was assessed using a mouse inhalation model. C. *neoformans* WT (n=10) or *Δaph1-1* (n=20) (5 x 10^5 fungal cells in 20 µl PBS) were inoculated intranasally in mice and observed daily for signs of ill-health. Mice which showed respiratory distress or which had lost 20% of their pre-infection weight, were deemed to have succumbed to the infection and were euthanized. A Kaplan Meier log rank test was then performed. However, the difference in median survival was not statistically significant (P=0.163).

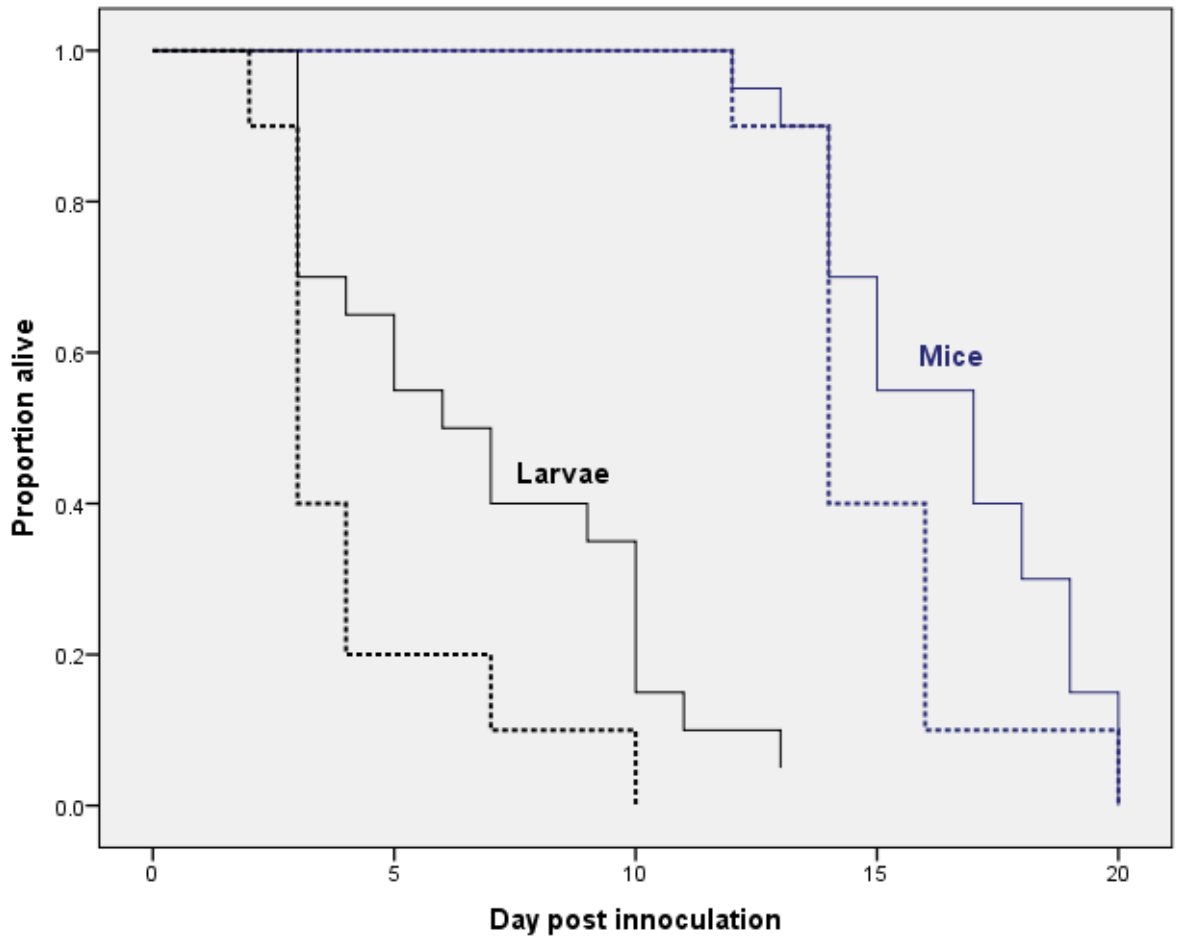

Figure 3.15 Combined survival analysis.

A log rank test stratified by species was performed using WT and *Δaph1-1* data from both the larval and mouse study (Figure 3.13 and 3.14). This combined analysis performed with the assistance of statistician Karen Bythe (Western Sydney Local Health District) demonstrated a statistically significant difference between WT and *Δaph1-1* (P=0.012).

3.10 Investigating potential mechanisms of Aph1 contribution to *C. neoformans* virulence: Role of Aph1 in adhesion of Cryptococci to lung epithelium

Previous studies by (Collopy-Junior *et al*., 2006) measured the effect of inhibitors of acid phosphatase on the attachment of *C. neoformans* to kidney epithelial cells and demonstrated that fungi with irreversibly inhibited acid phosphatase activity are less capable of adhering to these cells. A potential problem with this approach is that acid phosphatase inhibitors are non-specific. In this section, a more direct approach is used to assess the effect

of secreted Aph1 activity on fungal adherence: by determining the extent of binding of WT and *Δaph1-1* to a monolayer of the lung epithelial cell line, A549, using colony counting (2.12). The results in Figure 3.16 indicate that there is no significant difference between the binding of WT and *Δaph1-1* to lung epithelial cells.

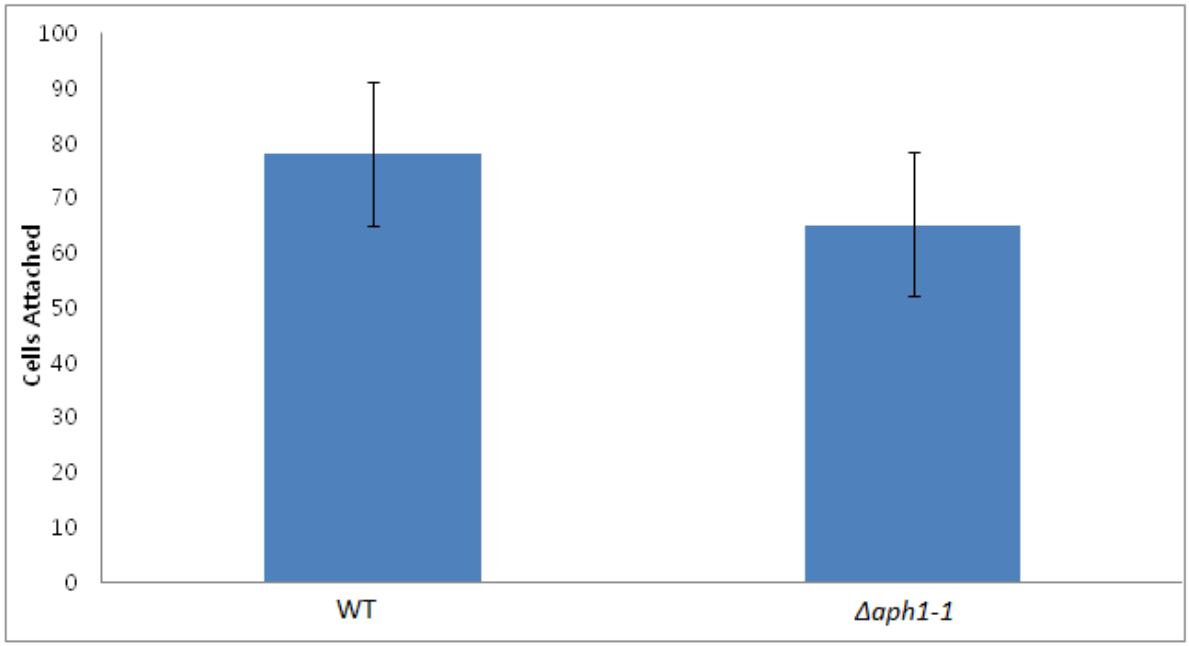

Figure 3.16 Attachment of WT and *Δaph1-1* fungal cells to a lung epithelial cell line.
A549 Cryptococcus strains were grown overnight in MM-KCl (low phosphate, Aph1 inducing media). The cells were counted and resuspended in the 2 day-old (spent) A549 cell culture medium rather than fresh medium to ensure that phosphate levels remain depleted and, hence, secreted Aph1 levels high. After co-incubation of *C. neoformans* and A549 cells, the unbound fungal cells were removed. The number of fungal cells that remained attached was determined by lysing the epithelial monolayer and plating the cryptococcal cells onto SAB plates, followed by counting of the colonies formed after 2 days incubation at 30°C. The results represent the mean and standard error of 3 biological replicates. This experiment was performed with the assistance of Dr Sophie Lev.

3.11 Determining whether the expression of *APH2*, *APH3* and *APH4* is phosphate-regulated and dependent on *APH1*

To determine whether the expression of *APH2*, *APH3* and *APH4* are also regulated by phosphate availability, the level of expression of each gene was compared in WT in the presence and absence of phosphate (Figure 3.17). In the absence of phosphate, the

expression of *APH2*, *APH3* and *APH4* increased, although not as considerably by 2.844-fold, 21.1-fold and 228.31-fold, respectively, compared to ~330 fold for *APH1* (Figure 3.7), confirming that expression of *APH3* and *APH4,* and to a much lesser extent *APH2,* is regulated by phosphate availability. Since Aph1 has a minor contribution to virulence in two animal models (Figure 13-15), it was hypothesized that, if functional redundancy exists among the APH family, expression of some/all acid phosphatase-encoding genes would increase above WT levels in the absence of Aph1 as a potential mechanism of compensation. To test this hypothesis, expression of *APH2*, *APH3* and *APH4* was tested in the *Δaph1-1* strain following incubation in Pi-deficient and Pi-replete media (Figure 3.17). While the expression of *APH3* and *APH4* and, to a lesser extent of *APH2*, was induced in *Δaph1-1* in the absence of Pi, it was not higher than in the WT strain.

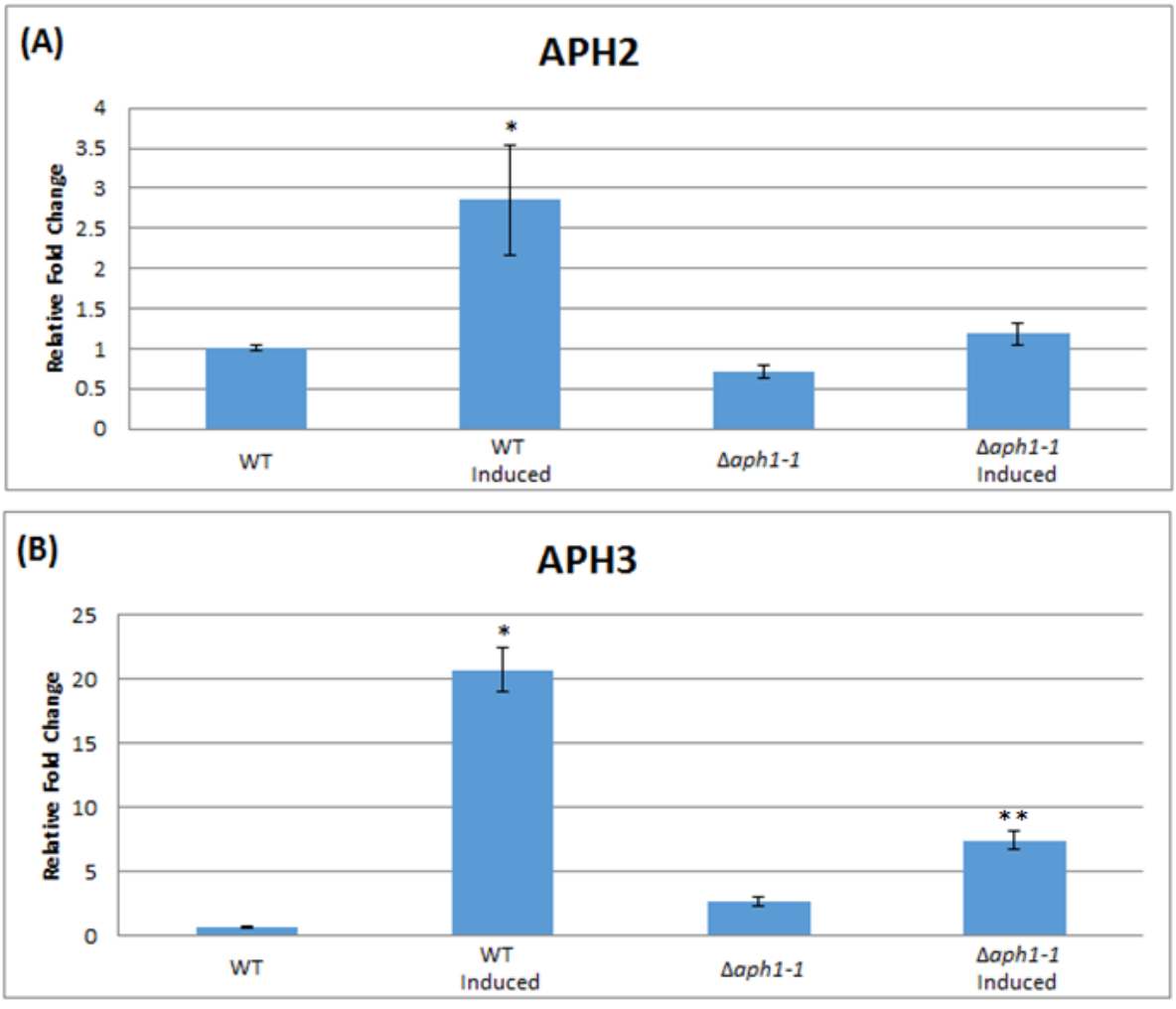

Continued on page 59

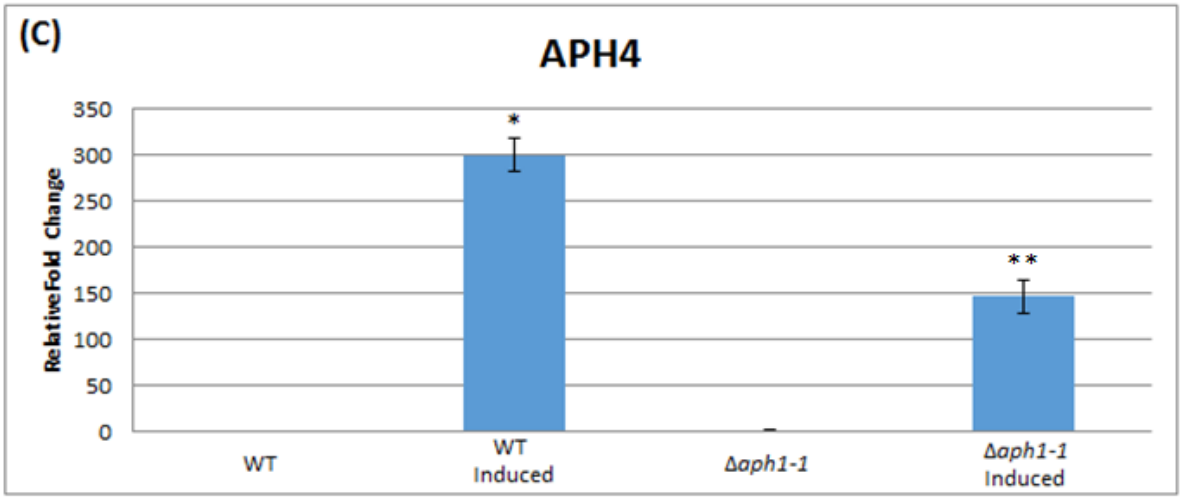

Figure 3.17 Expression of *APH2, APH3* and *APH4* in the presence and absence of phosphate in WT and *Δaph1-1* strains.

WT and Δ*aph1-1* were incubated for 3 hours under Pi-replete (non-inducing) or Pi-deficient (inducing) conditions, as in Figure 3.6. RNA was extracted and cDNA synthesized. *APH2,3,4* transcripts were quantified by qPCR using the ΔΔCt calculation method after normalizing against expression of the housekeeping gene actin 1 (*ACT1*). The experiment was conducted in 3 biological replicates with error bars indicating standard error. *Indicates that the increase in expression is statistically significant relative to all other samples ($p<0.05$). ** indicates that the increase in expression is statistically significant, relative to its non-induced control only, as determined using one-way ANOVA with a Tukey post-hoc test. Primer pairs used are indicated in section 2.13.4, Table 3.

4 Discussion

Extracellular acid phosphatase activity has been detected in a large proportion of *C. neoformans* strains isolated from patients with AIDS (Vidotto *et al*., 2006), suggesting that the enzyme(s) responsible play a role in cryptococcal virulence. The secreted acid phosphatase in the model non-pathogenic yeast, *Saccharomyces cerevisiae*, is Pho5, which contains a secretory leader peptide and is a component of the phosphate responsive (PHO) system (Figure 1.3). A major aim of this thesis was to identify the enzyme(s) responsible for extracellular acid phosphatase activity in the clinical *Cryptococcus neoformans* serotype A type strain, H99. A BLAST search of the *C. neoformans* database using the Pho5 protein sequence as a query identified four putative acid phosphatases, with only CNAG_02944 (Aph1) predicted to be secreted on the basis of the presence of a signal peptide (SP). Interestingly, the other acid phosphatases CNAG_06967 (Aph2) CNAG_02681 (Aph3) and CNAG_06115 (Aph4) do not contain a signal peptide and are therefore most likely to be intracellular. In support of this, our research group only identified Aph1 in a proteomic analysis of the H99 secretome (Lev *et al.*, 2014).

4.1 Phylogenetic analysis of fungal acid phosphatases

Phylogenetic analysis of fungal acid phosphatases demonstrates that Aph1 is most similar to Aph2 (59.5% similar, 40.3% identical) suggesting that one arose from the other by gene duplication. Gene duplication plays a key role in an organism's complexity, adaptation and diversification to closely related strains and species (Prince & Pickett, 2002) (Long *et al.*, 2003). It is also interesting to note that, similar to other fungal species, the cryptococcal acid phosphatase group includes extra- and intracellular members, indicating that these enzymes have functions both inside and outside the cell. The secreted acid phosphatase, Pho5, in *S. cerevisiae* shares 51.6% similarity and 19.86% identity with Aph1. Aph1 did not cluster with Pho5 in *S.cerevisiae*, even though it was found to be regulated in the same way. Interestingly cryptococcal acid phosphatases are relatively close to phytases from other fungal species, suggesting that IP_6 is a substrate and that acid phosphatases might play a role in inositol polyphosphate homeostasis. However, IP_6 was unable to be shown that it was a substrate of Aph1 as the malachite green assay reagent reacted with IP_6, forming a precipitate.

The other interesting observation from the cluster analysis is that only two of the cryptococcal acid phosphatases, Aph1 and Aph2, cluster together. This was despite the fact that *APH2* induction was not as phosphate-responsive as induction of the other *APH* genes (Figure 3.17). The result suggests that *APH1* and *APH2* may be less similar in their promoters than in their protein coding region. Possible reasons for the divergence of Aph1/Aph2 from Aph3 and Aph4 may be that they have evolved to have different roles and/or substrate specificities. Determining the substrate specificities of Aph2-4 in future studies will provide important information on the function of these enzymes. Clues about functional divergence can also be gained by comparing the subcellular location of each APH enzyme and whether any of the genes encoding the intracellular APH enzymes are upregulated in the absence of Aph1 (see below). Subcellular location has already been determined for Aph1 by attaching it to the DsRed fluorophor. Interestingly, it was shown that Aph1 is transported to vacuoles and to the cell periphery via endosomes (Lev *et al*., 2014). Aph1 therefore appears to have an intracellular and an extracellular role. The fact that *C. neoformans* produces many intracellular acid phosphatases suggests that they play important roles inside the cell, and that some functional redundancy might occur.

4.2 Aph1 production is regulated by phosphate availability and serves as a reporter for defining the PHO regulatory system in *C. neoformans*

After identifying that Aph1 is the only acid phosphatase in *C. neoformans* predicted to be secreted, the *APH1* gene was deleted using a targeted gene deletion strategy. Screening for genuine knockout strains was facilitated by the use of a colorimetric enzyme assay utilizing pNPP, which is converted to pNP by acid phosphatase. The screen identified 3 potential knockout clones, only two of which were certified to be genuine knockouts by PCR screening (*⊿aph1-1* and *⊿aph1-2*).

To address aims 2 and 3, the extracellular acid phosphatase activity produced by the WT and *Δaph1* strains in the presence and absence of phosphate was compared using the same colorimetric assay used in the knockout screening procedure. Acid phosphate activity was only detected in WT secretions in the absence of phosphate, but not in *Δaph1* secretions, proving that Aph1 is the sole acid phosphatase contributing to extracellular phosphatase activity and that its secretion is regulated by phosphate availability. Using qPCR, the regulation of secretion of Aph1 activity in a phosphate-depleted environment was

confirmed to occur at the level of transcription. Thus, even though Aph1 did not cluster closely to Pho5, which is also induced by phosphate deprivation, the results are consistent with Aph1 being the orthologue of Pho5, as the two proteins share a similar mode of regulation. Three high-affinity phosphate-repressible phosphate transporters (PHO 89, 840 and 84) have been identified in *C. neoformans* (Kretschmer *et al*., 2014) that could potentially allow the free phosphate generated by Aph1 to be incorporated into the cell to maintain the high levels required for normal intracellular function. These cryptococcal phosphate transporters are orthologues of Pho89 and Pho84 in *S. cerevisiae.*

In addition to the high-affinity phosphate transporters, (Kretschmer *et al*., 2014) also identified other probable regulatory components of the PHO system in *C. neoformans* based on their homology to PHO system components in *S. cerevisiae,* including the cyclin dependent kinase Pho85, the cyclin Pho80 and the cyclin-dependent kinase inhibitor Pho81*:* encoded by CNAG_07871, CNAG_01922 and CNAG_02541, respectively. Following activation by the Pho85-Pho80-Pho81 complex in *S. cerevisiae*, transcription factors Pho4 and Pho2 regulate expression of *PHO* genes involved in phosphate acquisition and storage (acid phosphatases, phosphate transporters and enzymes involved in the synthesis and degradation of polyphosphate). However the transcription factor equivalent(s) in *C. neoformans* remain to be identified. Since Aph1 can be used a reporter enzyme for activation of the poorly described PHO pathway in *C. neoformans,* detection of its activity using the chromogenic assay described in this thesis will allow the identification of PHO translational machinery in future studies using transcription factor knockout libraries.

4.3 Aph1 is not essential for growth of *C. neoformans* in the absence of an external source of phosphate

In addition to mobilizing phosphate from extracellular organic sources, Aph1 is likely to play a role in mobilizing intracellular phosphate from polyphosphate or disposable phosphoproteins with expired half-lives, as it has a dominant location in vacuoles (Lev *et al*., 2014). The vacuoles of fungal and plant cells are analogous to the lysosomes of mammalian cells and are involved in the storage of waste products, and phosphate as polyphosphate. Old proteins and other molecules are also broken down and recycled inside vacuoles. Thus the location of Aph1 in vacuoles and its ability to remove phosphate from a diverse array of molecules sent there for storage (in the case of polyphosphate) or breakdown and recycling

(in the case of phosphorylated and carbohydrate-modified proteins) suggests that Aph1 plays a role in fungal cellular phosphate homeostasis. Vacuoles are acidic and therefore provide a favourable environment for Aph1 to function. It would be interesting in future studies to determine whether polyphosphate is a substrate of Aph1 as this would provide evidence of a role for Aph1 in the release of phosphate from these vacuolar stores.

The growth rate of WT and *Δaph1* in the absence of phosphate was compared using a drop dilution assay (Figure 3.10). *Δaph1* grew at a similar rate to WT in the absence of phosphate, where growth of both strains is dependent on phosphate derived from intracellular stores such as vacuolar polyphosphates, phospholipids and nucleic acids, and organic phosphate sources such as phosphotyrosine, glucose-1-phosphate, mannose-6-phosphate, β-glycerol phosphate, AMP and ATP, which are substrates of Aph1 (Figure 3.8). This result suggests that intracellular Aph1 is not crucial for the ability of *C. neoformans* to mobilise Pi from intracellular phosphate sources to maintain phosphate homeostasis and support cryptococcal growth in an environment depleted of free phosphate. The putative role for intracellular Aph1 in phosphate mobilisation may not be essential for growth of *C. neoformans* in phosphate-deficient medium because the other APHs fullfill the role. Intracellular Aph3 and Aph4, and to a lesser extent Aph2, could potentially play a role in mobilising Pi from organic sources in the absence of Aph1. Phospholipids constitute a large proportion of cellular Pi, and bacteria, plants and some non-pathogenic fungi, such as *S. cerevisiae* and *Neurospora crassa*, have acquired the ability to replace phospholipids with non-phosphorous lipids when Pi is limited (Nakamura, 2013) (Benning *et al.*, 1995) (Lopez-Lara *et al.*, 2005) (Benning & Ohta, 2005) (Hartel *et al.*, 2000). The ability to form Pi-free lipids allows the freeing-up of Pi needed for growth and the maintenance of cellular Pi homeostasis. Cryptococcal genes encoding enzymes involved in releasing Pi from phospholipids will be tested for Pi responsiveness in future studies.

The growth rate of WT and *Δaph1* in the presence of the Aph1 substrates, β-glycerolphosphate or glucose-1-phosphate (Figure 3.8) as the sole source of phosphate, was also tested. Surprisingly, *Δaph1* grew at a similar rate to WT in the presence of two Aph1 substrates, β-glycerol phosphate or glucose-1-phosphate, provided as the sole source of phosphate. The ability of secreted Aph1 to make free phosphate available from these external organic sources therefore does not appear to be crucial to maintain phosphate homeostasis and support cryptococcal growth under these conditions. It is possible that in

the absence of secreted Aph1, β-glycerol phosphate and glucose-1-phosphate are transported into the cell for hydrolysis by intracellular APHs, or incorporation into cellular metabolism.

4.4 Aph1 hydrolyses a diverse range of substrates

An important functional characteristic of an enzyme is its substrate specificity. Depending on the range and type of substrate it is able to catalyse, assumptions can be made about its biological and physiological significance. Acid phosphatases are known to catalyse a wide range of substrates (Anand & Srivastava, 2012). So the next aim of the thesis was to determine the substrate specificity of Aph1. Aph1 was also found to hydrolyse a diverse range of substrates including sugars such as glucose-1-phosphate and mannose-6-phosphate, the lipid precursor β-glycerol phosphate, and the nucleotides adenosine triphosphate (ATP) and adenosine monophosphate (AMP), which are important for energy production, signaling and modulating the immune response. The results demonstrate that Aph1 can scavenge Pi from a wide range of organic phosphates. The only evidence of discriminatory hydrolysis of phosphate was among the amino acids. Aph1 demonstrated a strong preference for phosphotyrosine, but not for phosphothreonine or phosphoserine. Phosphotyrosine is likely to be present on proteins targeted to vacuoles for turnover and on signalling molecules. Similar to the nucleotides and sugars, tyrosine contains a bulky aromatic side chain whilst serine and threonine contain shorter aliphatic chains terminating with an alcohol (Figure 4.1). Except for β-glycerol phosphate, Aph1 displayed a preference for bulky aromatic side chains attached to phosphate. The finding in this thesis that phosphotyrosine is the preferred amino acid substrate for Aph1 is in contrast to the findings of (Collopy-Junior *et al*., 2006) who found that phosphothreonine was the best substrate of the extracellular acid phosphatase activity produced by *C. neoformans*, which we now know from this study is due to Aph1. A possible reason for the different result is that Collopy-Junior *et al* used sodium orthovanadate to inhibit extracellular acid phosphatase activity whereas in this study Aph1 was eliminated directly through gene deletion. Sodium orthovanadate is a non-specific irreversible inhibitor of acid phosphatase activity and may therefore have inhibited other important regulatory enzymes such as alkaline phosphatases. However, Collopy-Junior did show that β-glycerol phosphate is a potential substrate of acid phosphatase, and it was confirmed in this thesis that β-glycerol phosphate is indeed a

substrate of Aph1.

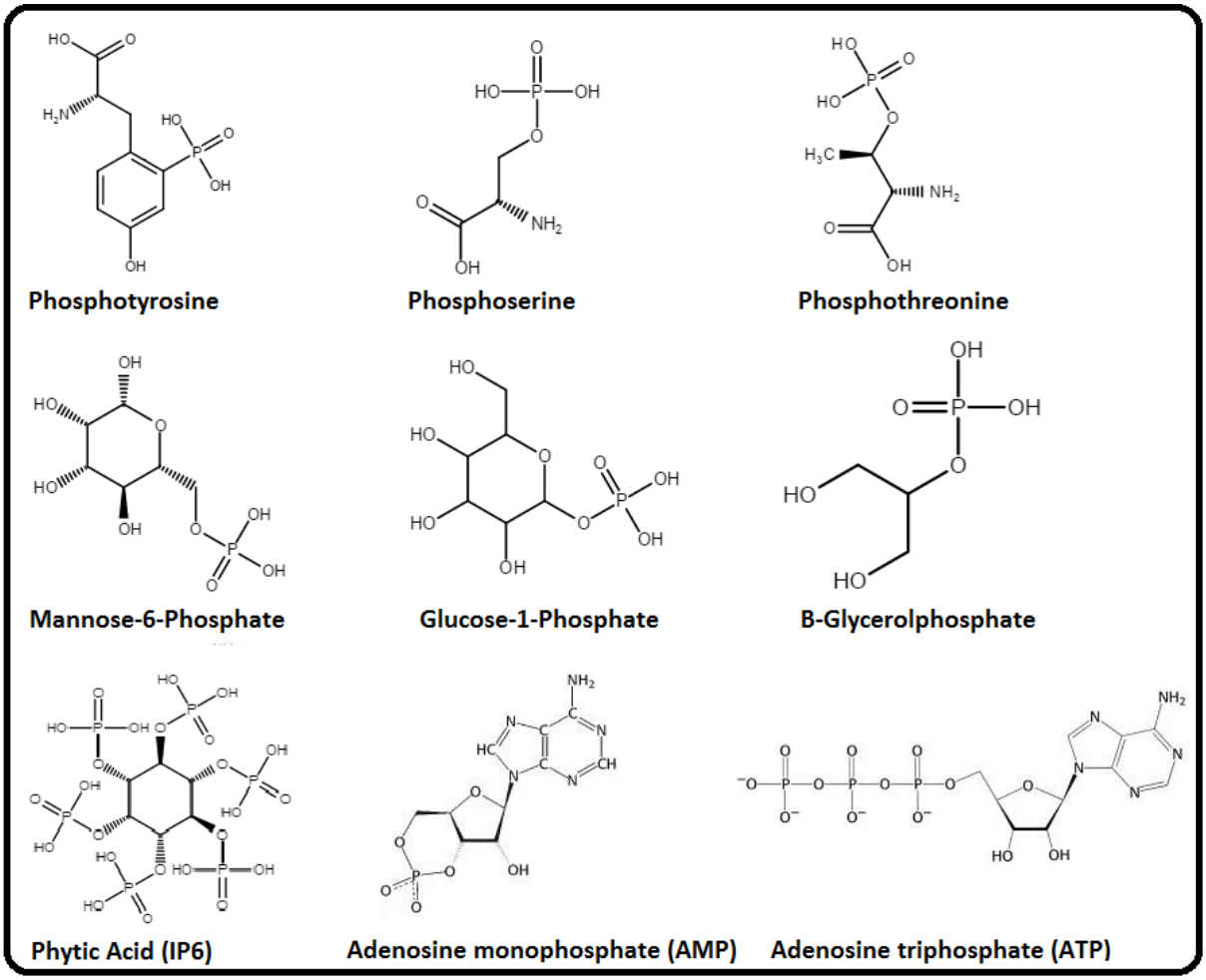

Figure 4.1 Chemical structure of the potential and confirmed Aph1 substrates.

All of the above were confirmed to be substrates of Aph1 except phosphoserine, phosphothreonine and phytic acid. Except for β-glycerol phosphate, Aph1 showed a strong preference for a bulky aromatic side chains attached to phosphate. Phytic acid (IP_6), which is also a bulky aromatic substrate, could not be tested in this thesis because the malachite green assay was not compatible. All structures were obtained from http://www.chemicalize.org/.

4.5 How does Aph1 contribute to the virulence of *C. neoformans?*

Aph1 was not essential for production of key virulence factors, cell wall integrity, growth at host temperature (37°C) or stress resistance (Figure 3.9). It was also not essential for growth under a combination of stresses (Figure 3.10). However, it was required for full virulence in animal models (Figure 3.13-3.15). A previous study by (Collopy-Junior *et al*.,

2006) demonstrated that adhesion of *C. neoformans* cells to an MA104 monkey kidney epithelial cell line was reduced following non-specific irreversible inhibition of acid phosphatase activity by sodium orthovanadate. Thus, the ability of WT and *Δaph1* to bind to a lung epithelial cell line was investigated. However, no difference in binding was found suggesting that Aph1 does not promote interaction of *C. neoformans* with host lung epithelium. A possible reason for the discrepancy between these results and those of (Collopy-Junior *et al*., 2006) is that, as mentioned above, sodium orthovanadate also inhibits other important regulatory enzymes in addition to Aph1, such as protein tyrosine phosphatases and alkaline phosphatases, which may promote fungal adherence in these studies. However it cannot be ruled out that another reason for the discrepancy in the results is that Collopy-Junior *et al* used a different cell line.

Kretschmer *et al*., 2014 showed that the loss of the high-affinity phosphate transporter system in *C. neoformans* via gene deletion attenuated the expression of the key virulence factors capsule and melanin, increased the susceptibility of *C. neoformans* to phosphate starvation and macrophage killing and attenuated the virulence of *C. neoformans* in a mouse model. (Fan *et al.*, 2005) demonstrated that the expression of high-affinity phosphate transporter was upregulated during macrophage infection with *C. neoformans*. Taken together, these studies demonstrate that the acquisition of phosphate from the host environment is essential for the virulence of *C. neoformans*. Our findings suggest that Aph1 is not required for the mobilization of phosphate from host-derived organic compounds to the extent that it impacts on growth and Pi homeostasis. However, the possibility cannot be ruled out that Aph1 hydrolyses a host-specific substrate other than glucose 1-phosphate or β-glycerol phosphate which is essential for achieving full virulence.

4.5.1 Host invasion *C. neoformans*, and most other fungi, play a major role in the breakdown of organic matter in the environment by secreting a diverse array of hydrolytic enzymes, including proteases, phospholipases and acid phosphatases. Some of these enzymes, including phospholipase B (PLB) and proteases are also secreted into the host to aid the invasion and dissemination of *C. neoformans*. Extracellular Aph1 may therefore play a role in allowing *C. neoformans* to invade host tissue potentially by modulating the surface of host cells via its dephosphorylation capability (Kiffer-Moreira *et al*., 2007a), (Kneipp *et al*., 2003, Kneipp *et al*., 2004) (Kneipp *et al*., 2012) (Fernanado *et al.*, 1999). However, since

Aph1, does not affect the binding of *C. neoformans* to a lung epthithelial cell line, it is unlikely that it plays a major role in aiding fungal invasion of the host. In the more advanced stages of infection, *C. neoformans* often forms cryptococcomas in lung and brain tissue, which are solid tumor-like masses, or granulomas which are clumps of cells embedded in a capsular matrix similar to a biofilm and surrounded by infiltrating monocytes. It has been demonstrated that the central regions of cryptococcomas are acidic and therefore provide a favorable environment for acid phosphatases to function.

4.5.2 Scavenging phosphate from the host environment One host environment that *C. neoformans* commonly encounters is the inside of the phagolysosome of macrophages, since these immune cells are able to phagocytose fungal cells (Geunes-Boyer *et al.*, 2009). There is evidence to suggest that the phagolysosome is low in free phosphate since the high affinity phosphate system is upregulated in *C. neoformans* cells during contact with macrophages (Fan *et al*., 2005). Mannose-6-phosphate, which was found to be a substrate of Aph1, serves as a recognition marker for targeting mammalian proteins to the lysosome and may provide a source of phosphate to *C. neoformans* growing inside macrophage phagolysosomes.

4.5.3 Modulation of the host immune system AMP and ATP were also found to be Aph1 substrates. Excessive adenosine generation by cryptococcal acid phosphatases may allow them to subvert the host immune system. *C. neoformans* could encounter host-derived ATP and AMP when infecting phagocytes or when growing extracellularly. In mammals extracellular adenosine generates a cascade of tissue responses (Hasko *et al.*, 2007) (Hasko & Pacher, 2012). Studies conducted in human and murine models confirmed that adenosine suppresses TNF-α production by monocytes and macrophages (Hasko *et al*., 2007). Pathogens such as *Staphylococcus aureus*, Enteropathogenic *Escherichia coli* and *Trichomonas vaginalis* possess surface ectonucleotidases that can cleave the phosphate off ATP, ADP and AMP, generating adenosine, providing a means for the pathogens to subvert the host immune system. In the same way the ability for *C. neoformans* to utilise AMP and ATP as Aph1 substrates may assist the fungus to thrive in the host by impeding macrophage and monocyte function.

4.5.4 Signalling The most predominant phosphorylation sites in eukaryotes occur on serine, threonine and tyrosine residues (Gomes *et al*., 2011) and phosphorylation and dephosphorylation at these sites is part of a cell's signalling network. Since Aph1 preferentially removes phosphate from tyrosine, it may play a role in modulating phosphotyrosine-dependent signalling pathways in the fungus as well as the host.

4.6 *APH3* and *APH4* are induced by Pi deprivation in WT but not to a greater extent in the absence of *APH1*.

The cluster analysis suggests that Aph1 and Aph2 are closely related and, therefore, could have overlapping functions that result in only a small reduction in virulence when one enzyme is missing. To determine whether all cryptococcal APH genes are induced by low phosphate and whether they may have overlapping functions, the expression of *APH2*, *APH3* and *APH4* in the presence and absence of phosphate was assessed by qPCR in WT and *Δaph1. APH3* and *APH4,* but not *APH2,* were highly induced in both WT and *Δaph1* during phosphate deprivation. However the level of induction of each enzyme in *Δaph1* did not exceed that of WT. Since A*PH2* is expressed regardless of the phosphate status of the cell, it could still potentially compensate for the absence of *APH1* by mobilizing Pi from intracellular sources, even if its level of expression is not elevated in the absence of Aph1. Alternatively, other genes and regulators within the PHO system may be responsible for mobilizing Pi and compensating for the absence of Aph1. Determining whether the APH enzymes have overlapping roles will require deletion of *APH2*, *APH3* and *APH4*, individually and in combination, and assessing the effect of these combination deletions on the virulence of *C. neoformans* in future studies.

4.7 Concluding remarks

In conclusion, Aph1 was found to be the major secreted acid phosphatase responsible for the extracellular acid phosphatase activity in the H99 strain isolated from a patient with AIDS. Aph1 production was found to be phosphate repressible at the level of *APH1* transcription. Aph1 was only found to play a minor role in the virulence of *C. neoformans,* which may be due to compensation from other APH enzymes and/or other unidentified gene products of the PHO system. If other APH enzymes compensate for the absence of Aph1, this compensation is not reflected by an increase in their gene

transcription. The way in which Aph1 contributes to the virulence of *C. neoformans* is most likely via its ability to release Pi from a broad range of physiological substrates, including potential immunomodulators, and to contribute to the maintenance of Pi homeostasis.

5 Appendices

Appendix 1

Media and buffers recipe Media/buffers	**Recipe**
Minimal medium w/o glucose (laccase inducing medium)	10µM $CuSO_4$, 10mM $MgSO_4.7H_20$, 29.4mM KH_2PO_4, 13mM glycine, 3.0µM thiamine-HCl
Minimal medium with glucose (laccase suppressing medium)	15mM glucose, 10mM $MgSO_4.7H_2O$, 29.4mM KH_2PO_4, 13mM glycine, 3.0µM thiamine-HCl
Minimal medium w/o phosphate (APH inducing medium)	0.5% KCl, 15mM glucose, 10mM $MgSO_4.7H_2O$, 13mM glycine, 3.0µM thiamine-HCl
Minimal medium with phosphate (APH suppressing medium)	0.5% KH_2PO_4, 15mM glucose, 10mM $MgSO_4.7H_2O$, 13mM glycine, 3.0µM thiamine-HCl
RPMI-1640 agar	10.4g/L RPMI-1640 reagent, 34.53g/L MOPS buffer, 18g/L glucose (pH 7.0). 0.3g/L L-glutamine, 15g/L bacto agar
TBS, 20X	1540mM Tris base, 2.8M NaCl, 540mM KCl (pH 8.0)
Tris-glycine transfer buffer	25 mM Tris base, 192 mM glycine, 20% methanol
YPD agar	50g/L YPD, 2% (w/v) bacto agar
YPD broth	50g/L YPD

Appendix 2

Manufacturers and suppliers of kits, chemicals, enzymes, and antibodies Product	**Product number**	**Manufacturer**	**Australian distributor**
100% Ethanol	9326410009756	Chem-Supply Pty Ltd, SA, AUS	VWR International, QLD, AUS
1 kb DNA ladder	Invitrogen Corporation, CA,	USA	Invitrogen Australia Pty.
Agarose Amresco Inc., OH, USA	Astral Scientific, NSW,	AUS	
Acetic acid	100015N	BDH Laboratory Supplies, NSW, AUS	VWR International, QLD, AUS
Acetone	9326410008384	Chem-Supply Pty Ltd, SA, AUS	VWR International, QLD, AUS
Amersham hyperfilm™ ECL	28-9068-35	GE Healthcare Ltd, UK	VWR International, QLD, AUS
Bacto™ agar	281210	Becton, Dickinson and Company, MD, USA	Becton, Dickinson and Company, NSW, AUS
Bacto™ Yeast Extract	212750	Becton, Dickinson and Company, MD, USA	Becton, Dickinson and Company, NSW, AUS
Bovine serum albumin (BSA)	-	Moregate Biotech, QLD, AUS	Moregate Biotech, QLD, AUS
Calcofluor-White (Fluorescent Brightener 28)	F3543	Sigma-Aldrich, MO, USA	Sigma-Aldrich, NSW, AUS
Chloroform	1024452500	Merck KGaA, Germany	VWR International, QLD, AUS
Congo Red	C6767	Sigma-Aldrich, MO, USA	Sigma-Aldrich, NSW, AUS
Copper II sulfate (CuSO4.5H20)	171-500G	Ajax Finechem, NSW, AUS	VWR International, QLD, AUS
dNTPs (2.5mM each)	4030	TaKaRa Bio Company	Scientifix Pty. Ltd.,

			VIC, AUS
Glass beads, acid washed	G8772-500G	Sigma-Aldrich, MO, USA	Sigma-Aldrich, NSW, AUS
Glucose (Anhyd)	14535 5LB	Affymetrix, Inc., OH, USA	In Vitro Technologies, VIC, AUS
Glycerol	0854-1L	Amresco Inc., OH, USA	Astral Scientific Pty, Ltd, NSW, AUS
Glycine	0167-1KG	Amresco Inc., OH, USA	Astral Scientific Pty, Ltd, NSW, AUS
Gold bead. 0.6 µm		Bio-Rad, NSW, AUS	
Hydrochloric acid (HCl) 36%	1367-500ML	Ajax Finechem, NSW, AUS	VWR International, QLD, AUS
Immobilon-P 0.45 µm transfer membrane (PVDF membrane)	IPVH00010	Millipore Corporation, MA, USA	Merck Millipore AUS Pty. Ltd., NSW, AUS
India Ink stain	261194	Becton, Dickinson and Company, MD, USA	Becton, Dickinson and Company, NSW, AUS
Isopropyl alcohol/2-propanol	I9516-500ML	Sigma-Aldrich, MO, USA	Sigma-Aldrich, NSW, AUS
Magnesium sulfate (MgSO4.7H2O)	10151	Merck Pty Ltd., VIC, AUS	Merck Pty Ltd., VIC, AUS
Methanol	M/4056/PB17	Fisher Scientific UK Ltd, UK	VWR International, QLD, AUS
Millex® 0.22µM filter	SLGP033RS	Millipore Corporation, MA, USA	Merck Pty. Ltd, VIC, AUS
M-MLV 5x Reaction Buffer	M531A	Promega Corporation, WI, USA	Promega Corporation, NSW, AUS
M-MLV RT	M170B	Promega Corporation, WI, USA	Promega Corporation, NSW, AUS
NuPAGE® 4-12% Bis-Tris Gel, 1.0mm, 12 well	NP0322BOX	Life Technologies Corporation, CA, USA	Life Technologies Corporation, VIC, AUS

Sample Buffer (4x)	-	Corporation, CA, USA	Corporation, CA, USA
Oligo (dT) (100µM) Primer	-	Integrated Technologies Inc., IA, USA	Integrated Technologies Inc., IA, USA
Peptone Bacteriological	LP0037	Oxoid Ltd, England, UK	Thermo Fisher Scientific, VIC, AUS
Phenol red	6614	Hopkin and Williams Ltd, England, UK	-
Platinum® SYBR® Green qPCR SuperMix-UDG	11733-046	Life Technologies Corporation, CA, USA	Thermo Fisher Scientific, VIC, AUS
Ponceau	P3504-10G	Sigma-Aldrich, MO, USA	Sigma-Aldrich, NSW, AUS
Potassium chloride (KCl)	P9333-500G	Sigma-Aldrich, MO, USA	Sigma-Aldrich, NSW, AUS
Potassium dihydrogen ortho-phosphate (KH2PO4)	391-500G	Ajax Finechem, NSW, AUS	VWR International, QLD, AUS
RPMI-1640 Medium	R7755-10L	Sigma-Aldrich, MO, USA	Sigma-Aldrich, NSW, AUS
RQ1 DNase Stop Solution	M199A	Promega Corporation, WI, USA	Promega Corporation, NSW, AUS
RQ1 RNase-Free DNase	M610A	Promega Corporation, WI, USA	Promega Corporation, NSW, AUS
Promega kit Spin Miniprep Kit		Promega Corporation, WI, USA	Promega Corporation, NSW, AUS
Sabouraud Dextrose (SAB) agar plates	-		Media Room, CIDM, ICPMR, Westmead Hospital, Westmead
Sodium acetate (Anhyd)	679-500G	Ajax Finechem, NSW, AUS	VWR International, QLD, AUS
Sodium carbonate (Na2CO3)	463-500G	Ajax Finechem, NSW, AUS	VWR International, QLD, AUS
Sodium chloride (NaCl)	102414J	BDH Laboratory Supplies, NSW, AUS	VWR International, QLD, AUS
Sodium dodecyl sulfate (SDS)	0227-1KG	Amresco Inc., OH, USA	Astral Scientific Pty, Ltd, NSW, AUS
Sodium hydoxide (NaOH)	S5881-500G	Sigma-Aldrich, MO, USA	Sigma-Aldrich, NSW, AUS
Sodium phosphate dibasic (Na2HPO4)	S7907	Sigma-Aldrich, MO, USA	Sigma-Aldrich, NSW, AUS
Sodium phosphate monobasic monohydrate	S9638	Sigma-Aldrich, MO, USA	Sigma-Aldrich, NSW, AUS

(NaH2PO4.H20)			
SYBR Safe DNA gel stain	(10,000 e DNA gel	Invitrogen Corporation, CA,	USA
Invitrogen Australia Pty.	Ltd., VIC, AUS	Sorbitol	Sigma-Aldrich, MO, USA
Sigma-Aldrich Pty. Ltd.,	NSW, AUS	SuperScript III First-Strand	Synthesis System for RTPCR
Ex Taq polymerase		Takara Bio Inc., Japan	Scientifix, VIC, AUS
Thiamine Hydrochloride	T4625-5G	Sigma-Aldrich, MO, USA	Sigma-Aldrich, NSW, AUS
Trichloroacetic acid	T6399-500G	Sigma-Aldrich, MO, USA	Sigma-Aldrich, NSW, AUS
Tris base	0497-1KG	Amresco Inc., OH, USA	Astral Scientific Pty, Ltd, NSW, AUS
Tris-borate-EDTA (TBE)		Sigma-Aldrich, MO, USA	Sigma-Aldrich Pty. Ltd., NSW, AUS
TRIZOL® Reagent	15596026	Life Technologies Corporation, CA, USA	Life Technologies Corporation, VIC, AUS
UltraPure™	10977-023	Life Technologies	Life Technologies
DNase/RNase-Free Distilled Water	Corporation, CA, USA	Corporation, VIC, AUS	
Yeast Extract Peptone Dextrose (YPD) Broth	75858	Affymetrix, Inc., OH, USA	In Vitro Technologies, VIC, AUS

6 Reference

Alspaugh, J.A., L.M. Cavallo, J.R. Perfect & J. Heitman, (2000) RAS1 regulates filamentation, mating and growth at high temperature of *Cryptococcus neoformans. Molecular microbiology* **36**: 352-365.

Anand, A. & P.K. Srivastava, (2012) A molecular description of acid phosphatase. *Applied biochemistry and biotechnology* **167**: 2174-2197.

Arnold, W.N., L.C. Mann, K.H. Sakai, R.G. Garrison & P.D. Coleman, (1986) Acid phosphatases of *Sporothrix schenckii*. *Journal of general microbiology* **132**: 3421-3432.

Baddley, J.W., D.C. Schain, A.A. Gupte, S.A. Lodhi, L.K. Kayler, J.P. Frade, S.R. Lockhart, T. Chiller, J.S. Bynon, Jr. & W.A. Bower, (2011) Transmission of *Cryptococcus neoformans* by Organ Transplantation. *Clinical infectious diseases : an official publication of the Infectious Diseases Society of America* **52**: e94-98.

Belanger, P.H., D.A. Johnston, R.A. Fratti, M. Zhang & S.G. Filler, (2002) Endocytosis of *Candida albicans* by vascular endothelial cells is associated with tyrosine phosphorylation of specific host cell proteins. *Cellular microbiology* **4**: 805-812.

Benning, C., Z.H. Huang & D.A. Gage, (1995) Accumulation of a novel glycolipid and a betaine lipid in cells of *Rhodobacter sphaeroides* grown under phosphate limitation. *Archives of biochemistry and biophysics* **317**: 103-111.

Benning, C. & H. Ohta, (2005) Three enzyme systems for galactoglycerolipid biosynthesis are coordinately regulated in plants. *The Journal of biological chemistry* **280**: 2397-2400.

Bernard, M., I. Mouyna, G. Dubreucq, J.P. Debeaupuis, T. Fontaine, C. Vorgias, C. Fuglsang & J.P. Latge, (2002) Characterization of a cell-wall acid phosphatase (PhoAp) in *Aspergillus fumigatus*. *Microbiology* **148**: 2819-2829.

Casadevall, A., A.L
. Rosas & J.D. Nosanchuk, (2000) Melanin and virulence in *Cryptococcus neoformans*. *Current opinion in microbiology* **3**: 354-358.

Casadevall, A.J.R.P., (1998) *Cryptococcus neoformans*. ASM Press, Washington, DC.

Chau, T.T., N.H. Mai, N.H. Phu, H.D. Nghia, L.V. Chuong, D.X. Sinh, V.A. Duong, P.T. Diep, J.I. Campbell, S. Baker, T.T. Hien, D.G. Lalloo, J.J. Farrar & J.N. Day, (2010) A prospective descriptive study of cryptococcal meningitis in HIV uninfected patients in Vietnam - high prevalence of *Cryptococcus neoformans var grubii* in the absence of underlying disease. *BMC infectious diseases* **10**: 199.

Chayakulkeeree, M., T.C. Sorrell, A.R. Siafakas, C.F. Wilson, N. Pantarat, K.J. Gerik, R. Boadle & J.T. Djordjevic, (2008) Role and mechanism of phosphatidylinositol-specific phospholipase C in survival and virulence of *Cryptococcus neoformans*. *Molecular microbiology* **69**: 809-826.

Chen, S.C., L.C. Wright, J.C. Golding & T.C. Sorrell, (2000) Purification and characterization of secretory phospholipase B, lysophospholipase and lysophospholipase/transacylase from a virulent strain of the pathogenic fungus *Cryptococcus neoformans*. *The Biochemical journal* **347**: 431-439.

Chi, H., X. Yang, P.D. Kingsley, R.J. O'Keefe, J.E. Puzas, R.N. Rosier, S.B. Shears & P.R. Reynolds, (2000) Targeted deletion of Minpp1 provides new insight into the activity of multiple inositol polyphosphate phosphatase in vivo. *Molecular and cellular biology* **20**: 6496-6507.

Collopy-Junior, I., F.F. Esteves, L. Nimrichter, M.L. Rodrigues, C.S. Alviano & J.R. Meyer-Fernandes, (2006) An ectophosphatase activity in *Cryptococcus neoformans*. *FEMS yeast research* **6**: 1010-1017.

Djordjevic, J.T., (2010) Role of phospholipases in fungal fitness, pathogenicity, and drug development - lessons from *Cryptococcus neoformans*. *Frontiers in microbiology* **1**: 125.

Djordjevic, J.T., M. Del Poeta, T.C. Sorrell, K.M. Turner & L.C. Wright, (2005) Secretion of cryptococcal phospholipase B1 (PLB1) is regulated by a glycosylphosphatidylinositol (GPI) anchor. *The Biochemical journal* **389**: 803-812.

Doering, T.L., (2009) How sweet it is! Cell wall biogenesis and polysaccharide capsule formation in *Cryptococcus neoformans*. *Annual review of microbiology* **63**: 223-247.

Falkow, S., (1988) Molecular Koch's postulates applied to microbial pathogenicity. *Reviews of infectious diseases* **10 Suppl 2**: S274-276.

Fan, W., P.R. Kraus, M.J. Boily & J. Heitman, (2005) *Cryptococcus neoformans* gene expression during murine macrophage infection. *Eukaryotic cell* **4**: 1420-1433.

Fernanado, P.H., G.J. Panagoda & L.P. Samaranayake, (1999) The relationship between the acid and alkaline phosphatase activity and the adherence of clinical isolates of *Candida parapsilosis* to human buccal epithelial cells. *APMIS : acta pathologica, microbiologica, et immunologica Scandinavica* **107**: 1034-1042.

Fleisig, H., A. El-Din El-Husseini & S.R. Vincent, (2004) Regulation of ErbB4 phosphorylation and cleavage by a novel histidine acid phosphatase. *Neuroscience* **127**: 91-100.

Fries, B.C., S.C. Lee, R. Kennan, W. Zhao, A. Casadevall & D.L. Goldman, (2005) Phenotypic switching of *Cryptococcus neoformans* can produce variants that elicit increased intracranial pressure in a rat model of cryptococcal meningoencephalitis. *Infection and immunity* **73**: 1779-1787.

Fyfe, M., L. MacDougall, M. Romney, M. Starr, M. Pearce, S. Mak, S. Mithani & P. Kibsey, (2008) Cryptococcus gattii infections on Vancouver Island, British Columbia, Canada: emergence of a tropical fungus in a temperate environment. *Canada communicable disease report = Releve des maladies transmissibles au Canada* **34**: 1-12.

Garcia-Rodas, R., A. Casadevall, J.L. Rodriguez-Tudela, M. Cuenca-Estrella & O. Zaragoza, (2011) *Cryptococcus neoformans* capsular enlargement and cellular gigantism during Galleria mellonella infection. *PloS one* **6**: e24485.

Geunes-Boyer, S., T.N. Oliver, G. Janbon, J.K. Lodge, J. Heitman, J.R. Perfect & J.R. Wright, (2009) Surfactant protein D increases phagocytosis of hypocapsular *Cryptococcus neoformans* by murine macrophages and enhances fungal survival. *Infection and immunity* **77**: 2783-2794.

Ghannoum, M.A., (2000) Potential role of phospholipases in virulence and fungal pathogenesis. *Clinical microbiology reviews* **13**: 122-143, table of contents.

Ghannoum, M.A. & L.B. Rice, (1999) Antifungal agents: mode of action, mechanisms of resistance, and correlation of these mechanisms with bacterial resistance. *Clinical microbiology reviews* **12**: 501-517.

Gomes, M.T., A.H. Lopes & J.R. Meyer-Fernandes, (2011) Possible roles of ectophosphatases in host-parasite interactions. *Journal of parasitology research* **2011**: 479146.

Guerrero, A. & B.C. Fries, (2008) Phenotypic switching in *Cryptococcus neoformans* contributes to virulence by changing the immunological host response. *Infection and immunity* **76**: 4322-4331.

Hartel, H., P. Dormann & C. Benning, (2000) DGD1-independent biosynthesis of extraplastidic galactolipids after phosphate deprivation in Arabidopsis. *Proceedings of the National Academy of Sciences of the United States of America* **97**: 10649-10654.

Hasko, G. & P. Pacher, (2012) Regulation of macrophage function by adenosine. *Arteriosclerosis, thrombosis, and vascular biology* **32**: 865-869.

Hasko, G., P. Pacher, E.A. Deitch & E.S. Vizi, (2007) Shaping of monocyte and macrophage function by adenosine receptors. *Pharmacology & therapeutics* **113**: 264-275.

Hull, C.M. & J. Heitman, (2002) Genetics of *Cryptococcus neoformans*. *Annual review of genetics* **36**: 557-615.

Jain, N., A. Guerrero & B.C. Fries, (2006a) Phenotypic switching and its implications for the pathogenesis of *Cryptococcus neoformans*. *FEMS yeast research* **6**: 480-488.

Jain, N., L. Li, D.C. McFadden, U. Banarjee, X. Wang, E. Cook & B.C. Fries, (2006b) Phenotypic switching in a *Cryptococcus neoformans* variety *gattii* strain is associated with changes in virulence and promotes dissemination to the central nervous system. *Infection and immunity* **74**: 896-903.

Jarvis, J.N., A. Percival, S. Bauman, J. Pelfrey, G. Meintjes, G.N. Williams, N. Longley, T.S. Harrison & T.R. Kozel, (2011) Evaluation of a novel point-of-care cryptococcal antigen test on serum, plasma, and urine from patients with HIV-associated cryptococcal meningitis. *Clinical infectious diseases : an official publication of the Infectious Diseases Society of America* **53**: 1019-1023.

Kiffer-Moreira, T., A.A. de Sa Pinheiro, W.S. Alviano, F.M. Barbosa, T. Souto-Padron, L. Nimrichter, M.L. Rodrigues, C.S. Alviano & J.R. Meyer-Fernandes, (2007a) An ectophosphatase activity in *Candida parapsilosis* influences the interaction of fungi with epithelial cells. *FEMS yeast research* **7**: 621-628.

Kiffer-Moreira, T., A.A. Pinheiro, M.R. Pinto, F.F. Esteves, T. Souto-Padron, E. Barreto-Bergter & J.R. Meyer-Fernandes, (2007b) Mycelial forms of *Pseudallescheria boydii* present ectophosphatase activities. *Archives of microbiology* **188**: 159-166.

Klock, C., M. Cerski & L.Z. Goldani, (2009) Histopathological aspects of neurocryptococcosis in HIV-infected patients: autopsy report of 45 patients. *International journal of surgical pathology* **17**: 444-448.

Kneipp, L.F., A.S. Magalhaes, E.A. Abi-Chacra, L.O. Souza, C.S. Alviano, A.L. Santos & J.R. Meyer-Fernandes, (2012) Surface phosphatase in *Rhinocladiella aquaspersa*: biochemical properties and its involvement with adhesion. *Medical mycology* **50**: 570-578.

Kneipp, L.F., V.F. Palmeira, A.A. Pinheiro, C.S. Alviano, S. Rozental, L.R. Travassos & J.R. Meyer-Fernandes, (2003) Phosphatase activity on the cell wall of *Fonsecaea pedrosoi*. *Medical mycology* **41**: 469-477.

Kneipp, L.F., M.L. Rodrigues, C. Holandino, F.F. Esteves, T. Souto-Padron, C.S. Alviano, L.R. Travassos & J.R. Meyer-Fernandes, (2004) Ectophosphatase activity in conidial forms of *Fonsecaea pedrosoi* is modulated by exogenous phosphate and influences fungal adhesion to mammalian cells. *Microbiology* **150**: 3355-3362.

Kraus, P.R., C.B. Nichols & J. Heitman, (2005) Calcium- and calcineurin-independent roles for calmodulin in *Cryptococcus neoformans* morphogenesis and high-temperature growth. *Eukaryotic cell* **4**: 1079-1087.

Kretschmer, M., E. Reiner, G. Hu, N. Tam, D.L. Oliveira, M. Caza, J.H. Yeon, J. Kim, C.J. Kastrup, W.H. Jung & J.W. Kronstad, (2014) Defects in phosphate acquisition and

storage influence virulence of *Cryptococcus neoformans*. *Infection and immunity* **82**: 2697-2712.

Lenburg, M.E. & E.K. O'Shea, (1996) Signaling phosphate starvation. *Trends in biochemical sciences* **21**: 383-387.

Lev, S., B. Crossett, S.Y. Cha, D. Desmarini, C. Li, M. Chayakulkeeree, C.F. Wilson, P.R. Williamson, T.C. Sorrell & J.T. Djordjevic, (2014) Identification of Aph1, a Phosphate-Regulated, Secreted, and Vacuolar Acid Phosphatase in *Cryptococcus neoformans*. *mBio* **5**.

Loftus, B.J., E. Fung, P. Roncaglia, D. Rowley, P. Amedeo, D. Bruno, J. Vamathevan, M. Miranda, I.J. Anderson, J.A. Fraser, J.E. Allen, I.E. Bosdet, M.R. Brent, R. Chiu, T.L. Doering, M.J. Donlin, C.A. D'Souza, D.S. Fox, V. Grinberg, J. Fu, M. Fukushima, B.J. Haas, J.C. Huang, G. Janbon, S.J. Jones, H.L. Koo, M.I. Krzywinski, J.K. Kwon-Chung, K.B. Lengeler, R. Maiti, M.A. Marra, R.E. Marra, C.A. Mathewson, T.G. Mitchell, M. Pertea, F.R. Riggs, S.L. Salzberg, J.E. Schein, A. Shvartsbeyn, H. Shin, M. Shumway, C.A. Specht, B.B. Suh, A. Tenney, T.R. Utterback, B.L. Wickes, J.R. Wortman, N.H. Wye, J.W. Kronstad, J.K. Lodge, J. Heitman, R.W. Davis, C.M. Fraser & R.W. Hyman, (2005) The genome of the basidiomycetous yeast and human pathogen *Cryptococcus neoformans*. *Science* **307**: 1321-1324.

Long, M., E. Betran, K. Thornton & W. Wang, (2003) The origin of new genes: glimpses from the young and old. *Nature reviews. Genetics* **4**: 865-875.

Lopez-Lara, I.M., J.L. Gao, M.J. Soto, A. Solares-Perez, B. Weissenmayer, C. Sohlenkamp, G.P. Verroios, J. Thomas-Oates & O. Geiger, (2005) Phosphorus-free membrane lipids of *Sinorhizobium meliloti* are not required for the symbiosis with alfalfa but contribute to increased cell yields under phosphorus-limiting conditions of growth. *Molecular plant-microbe interactions : MPMI* **18**: 973-982.

McFadden, D., O. Zaragoza & A. Casadevall, (2006) The capsular dynamics of *Cryptococcus neoformans*. *Trends in microbiology* **14**: 497-505.

Meyer-Fernandes, J.R., M.A. da Silva-Neto, S. Soares Mdos, E. Fernandes, A.E. Vercesi & M.M. de Oliveira, (1999) Ecto-phosphatase activities on the cell surface of the amastigote forms of *Trypanosoma cruzi*. *Zeitschrift fur Naturforschung. C, Journal of biosciences* **54**: 977-984.

Mitchell, T.G., Perfect J.R., (1995) Cryptococcosis in the Era of AIDS—100 Years after the Discovery of *Cryptococcus neoforman*. *Clinical microbiology reviews* **8**: 515-548

Murray, P.R., Rosenthal, K. S. & Pfaller, M. A., (2009) *Medical Microbiology*. Mosby/Elsevier, Philadelphia.

Nakamura, Y., (2013) Phosphate starvation and membrane lipid remodeling in seed plants. *Progress in lipid research* **52**: 43-50.

Nichols, C.B., Z.H. Perfect & J.A. Alspaugh, (2007) A Ras1-Cdc24 signal transduction pathway mediates thermotolerance in the fungal pathogen *Cryptococcus neoformans*. *Molecular microbiology* **63**: 1118-1130.

Nicola, A.M., E.J. Robertson, P. Albuquerque, S. Derengowski Lda & A. Casadevall, (2011) Nonlytic exocytosis of *Cryptococcus neoformans* from macrophages occurs in vivo and is influenced by phagosomal pH. *mBio* **2**.

Oshima, Y., (1997) The phosphatase system in *Saccharomyces cerevisiae*. *Genes & genetic systems* **72**: 323-334.

Park, B.J., K.A. Wannemuehler, B.J. Marston, N. Govender, P.G. Pappas & T.M. Chiller, (2009) Estimation of the current global burden of cryptococcal meningitis among persons living with HIV/AIDS. *Aids* **23**: 525-530.

Persson, B.L., J.O. Lagerstedt, J.R. Pratt, J. Pattison-Granberg, K. Lundh, S. Shokrollahzadeh & F. Lundh, (2003) Regulation of phosphate acquisition in *Saccharomyces cerevisiae*. *Current genetics* **43**: 225-244.

Portela, M.B., L.F. Kneipp, I.P. Ribeiro de Souza, C. Holandino, C.S. Alviano, J.R. Meyer-Fernandes & R.M. de Araujo Soares, (2010) Ectophosphatase activity in *Candida albicans* influences fungal adhesion: study between HIV-positive and HIV-negative isolates. *Oral diseases* **16**: 431-437.

Pradel, E. & P.L. Boquet, (1991) Utilization of exogenous glucose-1-phosphate as a source of carbon or phosphate by *Escherichia coli* K12: respective roles of acid glucose-1-phosphatase, hexose-phosphate permease, phosphoglucomutase and alkaline phosphatase. *Research in microbiology* **142**: 37-45.

Prescott, L.M., Harley, J. P. & Klein, D. A., (2005) *Microbiology*. McGraw-Hill, New York.

Prince, V.E. & F.B. Pickett, (2002) Splitting pairs: the diverging fates of duplicated genes. *Nature reviews. Genetics* **3**: 827-837.

Pukkila-Worley, R., Q.D. Gerrald, P.R. Kraus, M.J. Boily, M.J. Davis, S.S. Giles, G.M. Cox, J. Heitman & J.A. Alspaugh, (2005) Transcriptional network of multiple capsule and melanin genes governed by the *Cryptococcus neoformans* cyclic AMP cascade. *Eukaryotic cell* **4**: 190-201.

Puri, R.V., P.V. Reddy & A.K. Tyagi, (2013) Secreted acid phosphatase (SapM) of *Mycobacterium tuberculosis* is indispensable for arresting phagosomal maturation and growth of the pathogen in guinea pig tissues. *PloS one* **8**: e70514.

Remaley, A.T., D.B. Kuhns, R.E. Basford, R.H. Glew & S.S. Kaplan, (1984) Leishmanial phosphatase blocks neutrophil O-2 production. *The Journal of biological chemistry* **259**: 11173-11175.

Rigden, D.J., (2008) The histidine phosphatase superfamily: structure and function. *The Biochemical journal* **409**: 333-348.

Saha, A.K., J.N. Dowling, A.W. Pasculle & R.H. Glew, (1988) *Legionella micdadei* phosphatase catalyzes the hydrolysis of phosphatidylinositol 4,5-bisphosphate in human neutrophils. *Archives of biochemistry and biophysics* **265**: 94-104.

Salas, S.D., J.E. Bennett, K.J. Kwon-Chung, J.R. Perfect & P.R. Williamson, (1996) Effect of the laccase gene CNLAC1, on virulence of *Cryptococcus neoformans*. *The Journal of experimental medicine* **184**: 377-386.

Shakarian, A.M., M.B. Joshi, E. Ghedin & D.M. Dwyer, (2002) Molecular dissection of the functional domains of a unique, tartrate-resistant, surface membrane acid phosphatase in the primitive human pathogen *Leishmania donovani*. *The Journal of biological chemistry* **277**: 17994-18001.

Shapiro, R.S., N. Robbins & L.E. Cowen, (2011) Regulatory circuitry governing fungal development, drug resistance, and disease. *Microbiology and molecular biology reviews : MMBR* **75**: 213-267.

Siafakas, A.R., T.C. Sorrell, L.C. Wright, C. Wilson, M. Larsen, R. Boadle, P.R. Williamson & J.T. Djordjevic, (2007) Cell wall-linked cryptococcal phospholipase B1 is a source of secreted enzyme and a determinant of cell wall integrity. *The Journal of biological chemistry* **282**: 37508-37514.

Siafakas, A.R., L.C. Wright, T.C. Sorrell & J.T. Djordjevic, (2006) Lipid rafts in *Cryptococcus neoformans* concentrate the virulence determinants phospholipase B1 and Cu/Zn superoxide dismutase. *Eukaryotic cell* **5**: 488-498.

Slavin, M., J. Fastenau, I. Sukarom, P. Mavros, S. Crowley & W.C. Gerth, (2004) Burden of hospitalization of patients with *Candida* and *Aspergillus* infections in Australia. *International journal of infectious diseases : IJID : official publication of the International Society for Infectious Diseases* **8**: 111-120.

Sun, L.M., T.Y. Chen, W.J. Chen, M.J. Hsieh, J.W. Liu, C.C. Huang & C.J. Wang, (2002) *Cryptococcus* infection in a patient with nasopharyngeal carcinoma: imaging findings mimicking pulmonary metastases. *The British journal of radiology* **75**: 275-278.

Tanaka, M., Y. Kishi, Y. Takanezawa, Y. Kakehi, J. Aoki & H. Arai, (2004) Prostatic acid phosphatase degrades lysophosphatidic acid in seminal plasma. *FEBS letters* **571**: 197-204.

Toffaletti, D.L., T.H. Rude, S.A. Johnston, D.T. Durack & J.R. Perfect, (1993) Gene transfer in *Cryptococcus neoformans* by use of biolistic delivery of DNA. *Journal of bacteriology* **175**: 1405-1411.

Tomar, P. & H. Sinha, (2014) Conservation of PHO pathway in ascomycetes and the role of Pho84. *Journal of biosciences* **39**: 525-536.

Vecchiarelli, A. & C. Monari, (2012) Capsular Material of *Cryptococcus neoformans*: Virulence and Much More. *Mycopathologia*.

Vidotto, V., S. Ito-Kuwa, K. Nakamura, S. Aoki, M. Melhem, K. Fukushima & E. Bollo, (2006) Extracellular enzymatic activities in *Cryptococcus neoformans* strains isolated from AIDS patients in different countries. *Revista iberoamericana de micologia* **23**: 216-220.

Voelz, K., S.A. Johnston, J.C. Rutherford & R.C. May, (2010) Automated analysis of cryptococcal macrophage parasitism using GFP-tagged cryptococci. *PloS one* **5**: e15968.

Waugh, M.S., C.B. Nichols, C.M. DeCesare, G.M. Cox, J. Heitman & J.A. Alspaugh, (2002) Ras1 and Ras2 contribute shared and unique roles in physiology and virulence of *Cryptococcus neoformans*. *Microbiology* **148**: 191-201.

Williamson, P.R., (1994) Biochemical and molecular characterization of the diphenol oxidase of *Cryptococcus neoformans*: identification as a laccase. *Journal of bacteriology* **176**: 656-664.

Wykoff, D.D. & E.K. O'Shea, (2001) Phosphate transport and sensing in *Saccharomyces cerevisiae*. *Genetics* **159**: 1491-1499.

Xander, P., A.F. Vigna, S. Feitosa Ldos, L. Pugliese, A.M. Bailao, C.M. Soares, R.A. Mortara, M. Mariano & J.D. Lopes, (2007) A surface 75-kDa protein with acid phosphatase activity recognized by monoclonal antibodies that inhibit *Paracoccidioides brasiliensis* growth. *Microbes and infection / Institut Pasteur* **9**: 1484-1492.

Zaragoza, O., M.L. Rodrigues, M. De Jesus, S. Frases, E. Dadachova & A. Casadevall, (2009) The capsule of the fungal pathogen *Cryptococcus neoformans*. *Advances in applied microbiology* **68**: 133-216.